AD-A189 815 LASER EVAPORATION STUDIES(U) ROCKWELL INTERNATIONAL 1/1
THOUSAND OAKS CA SCIENCE CENTER H O SANKUR OCT 87
SC5411 FR AFOSR-TR-87-1928 F49620-84-C-0091

UNCLASSIFIED F/G 20/12 NL

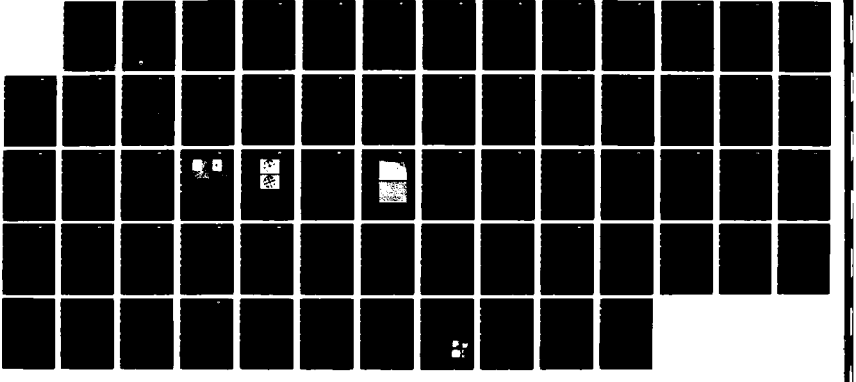

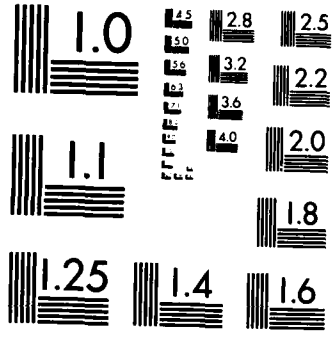

SC5411.FR

Copy No. 12

DTIC FILE COPY

LASER EVAPORATION STUDIES

Approved for public release;
distribution unlimited.

FINAL REPORT FOR THE PERIOD
September 1, 1984 through August 31, 1987

CONTRACT NO. F49620-84-C-0091
PROJECT NO. 2306-B2

Prepared for

Air Force Office of Scientific Research
Directorate of Electronic & Material Sciences
Building 410
Bolling AFB, DC 20332

H.O. Sankur
Principal Investigator

OCTOBER 1987

The following views and conclusions contained in this document are those of the authors and should not be interpreted as necessarily representing the official policies or endorsements, either expressed or implied, of the Air Force Office of Scientific Research or the U.S. Government.

Approved for public release; distribution unlimited

Rockwell International
Science Center

UNCLASSIFIED

SECURITY CLASSIFICATION OF THIS PAGE

REPORT DOCUMENTATION PAGE

1a REPORT SECURITY CLASSIFICATION **UNCLASSIFIED**	1b. RESTRICTIVE MARKINGS
2a SECURITY CLASSIFICATION AUTHORITY	3. DISTRIBUTION/AVAILABILITY OF REPORT **Approved for public release; distribution unlimited**
2b CLASSIFICATION DOWNGRADING SCHEDULE	
4 PERFORMING ORGANIZATION REPORT NUMBER(S) **SC5411.FR**	5 MONITORING ORGANIZATION REPORT NUMBER(S) **AFOSR-TR- 87-1928**
6a NAME OF PERFORMING ORGANIZATION **ROCKWELL INTERNATIONAL Science Center** 6b OFFICE SYMBOL (If Applicable)	7a NAME OF MONITORING ORGANIZATION Same as 8a
6c ADDRESS (City, State and ZIP Code) **1049 Camino Dos Rios Thousand Oaks, CA 91360**	7b ADDRESS (City, State and ZIP Code) Same as 8c
8a NAME OF FUNDING SPONSORING ORGANIZATION **Air Force Office of Scientific Research** 8b OFFICE SYMBOL (If Applicable) NE	9 PROCUREMENT INSTRUMENT IDENTIFICATION NUMBER **CONTRACT NO. F49620-84-C-0091**
8c ADDRESS (City, State and ZIP Code) **Building 410 Bolling Air Force Base, DC 20332**	10 SOURCE OF FUNDING NOS PROGRAM ELEMENT NO: 61102F; PROJECT NO: 2306/[redacted]; TASK NO: B1; WORK UNIT NO:
11 TITLE (Include Security Classification) **LASER EVAPORATION STUDIES (U)**	
12 PERSONAL AUTHOR(S) **Sankur, H.O.**	
13a TYPE OF REPORT **Final Report**	13b TIME COVERED FROM **09/01/84** TO **08/31/87**
14 DATE OF REPORT (Yr., Mo., Day) **1987, OCTOBER**	15 PAGE COUNT **63**

16 SUPPLEMENTARY NOTATION

The following views and conclusions contained in this document are those of the authors and should not be interpreted as necessarily representing the official policies or endorsements, either expressed or implied, of the Air Force Office of Scientific Research or the U.S. Government.

17 COSATI CODES			18. SUBJECT TERMS (Continue on reverse if necessary and identify by block number)
FIELD	GROUP	SUB GR	

19 ABSTRACT (Continue on reverse if necessary and identify by block number)

The physics of vaporization of matter under pulsed CO_2 laser evaporation was studied. Analysis of the nature of the vapor plume in several materials indicated the presence of numerous excited species, neutral as well as ionized species, and ions with high kinetic energies. High quality films of refractory metal oxides and epitaxial films of Ge were deposited. The oxide materials were dense and crystalline and had high refractive index values, even when deposited on room temperature substrates. Ge films were epitaxial and single crystalline when deposited on Si substrates at 300°C. Study of the relationship of deposition conditions and film properties clearly indicated the beneficial role of the energetic ions in the film deposition. Special emphasis was given to the solution of the problem of particulates in the films.

20 DISTRIBUTION/AVAILABILITY OF ABSTRACT UNCLASSIFIED/UNLIMITED ☒ SAME AS RPT. ☐ DTIC USERS ☐	21 ABSTRACT SECURITY CLASSIFICATION **UNCLASSIFIED**
22a NAME OF RESPONSIBLE INDIVIDUAL CAPT MALLOY	22b TELEPHONE NUMBER (Include Area Code) (202) 767-4931
	22c OFFICE SYMBOL NE

DD FORM 1473, 83 APR EDITION OF 1 JAN 73 IS OBSOLETE

UNCLASSIFIED

SECURITY CLASSIFICATION OF THIS PAGE

TABLE OF CONTENTS

TABLE OF CONTENTS

LIST OF FIGURES

LIST OF FIGURES

LIST OF TABLES

FOREWORD

This is the final report for the program to study the underlying physics and range of applicability of laser-assisted evaporation for the deposition of optical thin films. Most of the work involved use of CO_2 lasers.

In this research program, the nature of laser-induced vapor over the solid and liquid sources has been analyzed in detail. The properties of thin films formed by the condensation and impact of this vapor on various substrates have been studied and related to the evaporation conditions. The role of energetic species in the vapor on film properties has been elucidated. Special emphasis was given to eliminating or reducing the density of particulates in thin films.

In the final phase of this program, different aspects and several possible solutions of the "splashing" effect or particulate problem were studied. This information was applied in the deposition of high quality dielectric films of TiO_2, HfO_2, Ta_2O_5 and CeO_2 ,in addition to ZrO_2 studied earlier. Epitaxial films of Ge on Si were deposited on relatively low temperature substrates by pulsed laser evaporation of liquid Ge sources.

The body of this report deals with the results obtained in the final phase of the program and overall assessment of this technique, its advantageous features and drawbacks or areas that need further study. Results from previous phases of the program will be briefly summarized in the general outline of the program achievements. A more detailed description of these results is presented in the Appendices. Important results from other investigations will be referred to, and a brief outline of theoretical models of the laser-matter interaction will also be given in order to present a more complete picture for this technique within the science and technology of thin film deposition.

ACKNOWLEDGEMENTS

The program was sponsored by AFOSR and monitored by Capt. K. Malloy. Their support and encouragement and fruitful discussions with Dr. Malloy are gratefully acknowledged. We are also grateful to W. Gunning for technical direction and discussions, and to J. DeNatale (TEM analysis), J. Nelson, D. Matthews and A. Pritt for technical collaborations.

1.0 INTRODUCTION

In this section the physics of laser-induced evaporation and thin film deposition are discussed. We begin with a brief history of the development of this technique.

1.1 Historical Perspective

The interaction of coherent radiation with materials has been studied theoretically and experimentally since the development of high power lasers a quarter century ago. Data obtained with many diverse materials, and under a broad range of laser parameters (e.g., wavelength), and conditions (e.g., power density) have resulted in understanding and formulation of successful physical models. These studies have been engendered by technical fields such as metal machining (cutting welding, heat treating), semiconductor processing (recrystallization, dopant activation, annealing) laser-induced damage, and fusion energy research. Strong interest in such diverse scientific fields as laser-formed plasmas, multiphoton phenomena, and phase transformations under ultrafast cooling and heating, also fostered research in this subject.

In this program, the subject of the laser-matter interaction has been studied from the standpoint of evaporation and optical thin film deposition. This particular area has also been studied, but sporadically and without persistence, since the availability of high power lasers.[1] There are three reasons for this lack of continuity: investigation of laser evaporation for film deposition under a broad range of conditions, and to many classes of materials including organics,[2] semiconductors,[3] metals[4] and dielectrics,[5] has prevented it from having a technical focus. Concurrent and successful developments in competing techniques such as MBE and MOCVD for semiconductors, and sputtering for dielectric materials, has diverted interest from the laser-assisted deposition technique. A further reason for its slow acceptance is the emission of particulates from the source material and difficulty in controlling the evaporation rate.

Recent progress in laser-assisted evaporation has stimulated a renewed interest in this technique. Some recent results include deposition of dense crystalline dielectrics,[5] including stoichiometric high temperature superconductor material,[6] of semiconductor superlattices with arbitrary potential barrier shapes,[7] leading to the promising field of band gap engineering, and high quality semiconductors[8] at low epitaxy temperatures.

1.2 Physics of Laser-Assisted Evaporation

Physical phenomenology during laser assisted evaporation of solids can be categorized depending on the laser power density. The chemical and physical transformations of the evaporating surface, as well as the nature of the evaporants, strongly depend on this parameter. These are summarized below for the low power ($< 10^6$ W/cm^2), intermediate ($< 10^8$ W/cm^2), and high power ($> 10^8$ W/cm^2) regimes.

Low Power Regime

This regime is accessible with most focussed cw lasers or pulsed lasers in the free running mode. Results from many investigations indicate that the evaporation is essentially thermal in nature, with some slight and subtle differences. Alkali fluoride films were found to have considerably better properties in ultraviolet range (185-350 nm)[9] and different crystalline orientation when compared to films deposited by e-beam or thermal evaporation. (The results on alkali halide films were obtained under IR&D programs to develop cw laser assisted evaporation as a thin film deposition technique.) The advantages of using low power laser evaporation are the preservation of the source purity, surface heating, compatibility with reactive environments and minimal heat loading of the deposition chamber. These properties are also common to evaporation at higher power regimes. Evaporation from a small surface zone prevents reaction with the source container, thus avoiding contamination. The absence of hot filaments makes it possible to use a high pressure reactive gas environment. Finally, there is less heat radiation from the source in this deposition technique than in conventional evaporative methods.

Intermediate Power Regime

This range of power density is accessible with low power Q switched and focussed lasers in the free running mode. In this regime, photonic effects such as multiphoton absorption with bond breaking, free carrier generation, and ionization occur. The resultant vapor has dissociated and ionized species.[10] The release of this extrathermal energy at the thin film growth surface produces superior structural and electronic properties at lower substrate temperatures than required in conventional techniques.[8]

High Power Regime

This regime, accessible by high output pulsed lasers and focussed beams, holds the most promise for laser-assisted evaporation as a novel deposition technique with unique advantages. In this regime, high densities of ionized, excited state, atomic and high kinetic energy species are generated. Ultraviolet radiation, and even soft x-ray radiation, is also present. The high electric field of the laser beam at the solid surface causes dielectric breakdown and generation of a dense plasma with a temperature of ~ 10,000K (~ 7.5 eV). Laser radiation is absorbed by this plasma leading to a self-regulating regime. Here, the opacity of the plasma is such that laser radiation is blocked and only enough reaches the evaporation surface to replenish the plasma. The expansion of this plasma cloud in vacuum causes the species to assume large velocities (10-1000 times the thermal velocities encountered during evaporation). Decay of the excited and ionized species gives rise to photons in the UV and visible range.[11-14]

These energetic species play a crucial role in the formation of a dense and crystalline structure in thin films. The mechanisms in the interaction of energetic species with the film surface are probably similar to those that account for the effects observed in ion-assisted deposition. These include enhanced adatom mobility, breaking of weak bonds, and generation of nucleation centers.[15]

1.3 Deposition of Thin Films

The condensation of the vapor on a substrate to form a thin film is akin to that in other conventional evaporative techniques, but with some important differences. These differences, and the properties of laser-induced evaporation that give rise to these differences, are explained in Table 1.

Pulsed heating leads to congruent evaporation. The rapid heating of the material during the short pulses, and its rapid cooling due to the small volume of the heated zone embedded in the cooler source, prevent fractionation of the source material, even when the constituents have very different vapor pressures. The temperature cycle is short compared to the thermal diffusion time of the material.

High velocity species promote film crystallinity and denser packing because of enhanced adatom mobility and breaking of weak bonds.

Table 1

Properties of Pulsed Laser Evaporation

Property	Effect on Film Properties
Congruent evaporation	Stoichiometry
High kinetic energy species	Crystalline structure, sputtering of light atoms
High instantaneous evaporation rates	Low background gas incorporation crystalline structure
Plume in a narrow cone directed normal to the surface of the source	Thickness uniformity
Low power input, local evaporation	Low thermal radiation and degassing preservation of source purity
Particulate emission*	Degradation of optical, electrical properties

*This feature and solutions to this problem will be discussed in Section 3.2.1.

High velocity species also make it possible to use higher pressure reactive environments than is possible in conventional techniques. This is brought about by reduced interaction cross section of colliding particles with high relative velocities.

Energy in the vapor atoms, in the form of chemical dissociation of molecular species or ionization, also is released at the surface and is thought to improve the structure of the film.[8]

High rates of evaporation that can be obtained with high power lasers and high vapor pressure materials can be beneficial in altering the film properties. This is due to the release of heat of condensation in a thin surface layer. This thin layer consists of the newly deposited layer thickness and a characteristic thermal diffusion distance ($\sqrt{Dt}$) into the film. Here D is the heat diffusivity and t is the time of pulsed deposition. This time is taken as the pulse width, which is about 1 microsecond for TEA-CO_2 laser. Thus, for the duration of the deposition pulse, higher surface temperatures are obtained due to the release of heat of condensation. An additional benefit of high rates of evaporation is the low degree of background gas incorporation in the film material during the deposition. This means higher effective vacuum during thin film growth.

2.0 EXPERIMENTAL

The laser used in our experiments was a Lumonics model 820 TEA-CO_2 laser with a maximum output of 3 J/pulse. Antireflection coated ZnSe lenses were used to focus the laser beam onto evaporation sources. The resulting energy density or fluence, after taking losses in the mirrors and windows into account, was in the 10-160 J/cm^2 range.

The materials studied were principally metal oxide dielectrics, fluorides, zinc chalcogenides, and Ge.

The nature of the evaporants was analyzed in vacuum using optical techniques to analyze the emission spectrum and electrical probes to analyze the energy and velocity of the charged species. The experimental details are described in Appendix 6.0. A schematic of the experimental apparatus is shown in Fig. 1.

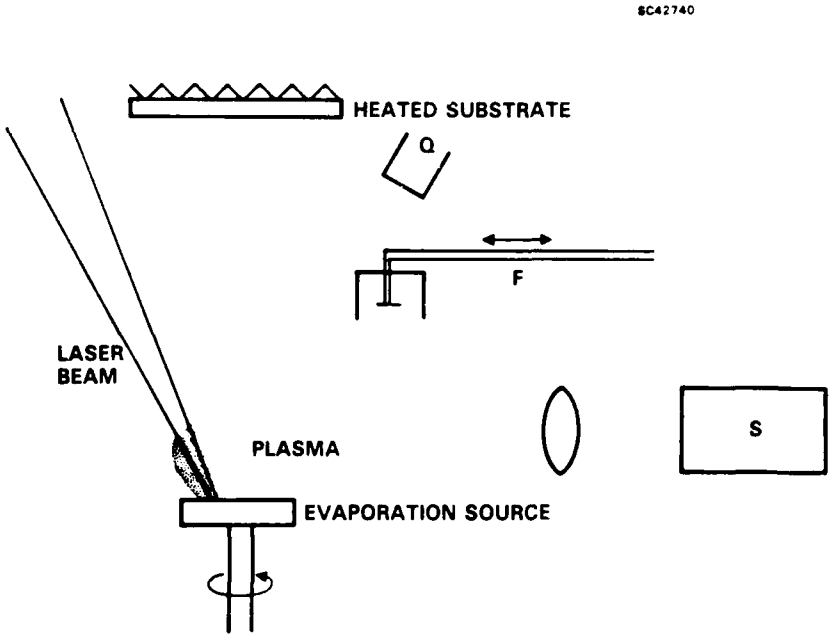

Fig. 1 Experimental apparatus for evaporant analysis. F, Faraday cup; Q, quartz thickness monitor; S, spectral monitor (i.e., optical multichannel analyzer).

Thin films were deposited on substrates of Si, glass, quartz, cleaved NaCl and sapphire. These, with the exception of NaCl, were cleaned with organic solvents, HCl-HNO_3, and O_2 plasma cleaning prior to deposition. The film thickness was in the 0.1-2 micron range.

The films were analyzed by transmission electron microscopy (TEM) for grain size, orientation, and crystalline phases. This was complemented by X-ray diffraction for thick films. The optical properties were determined by ellipsometry (thin films) and by spectroscopy and computer curve fitting of the data (thick films). All optical constant data reported in this report are at a wavelength of 632.8 nm. Surface morphology was studied by optical and scanning electron microscopies.

3.0 RESULTS

3.1 Summary of Previously Reported Results

Detailed account of these results are found in Appendices 6.1-6.3.

3.1.1 Plasma Emission Analysis

Spectral analysis of the plasma in the evaporant plume indicated that there were numerous states of excitation and ionization of the atomic species (Fig. 2). For metal oxides, excited states of neutral, as well as singly, doubly, and even triply ionized metal and oxygen species, were observed. Analysis of emission intensity data, assuming local thermal equilibrium in the plasma, indicated that the plasma temperature was ~ 6000°C for Al_2O_3 and SiO_2. This value agrees well with data reported by other investigators for other materials under similar power densities.

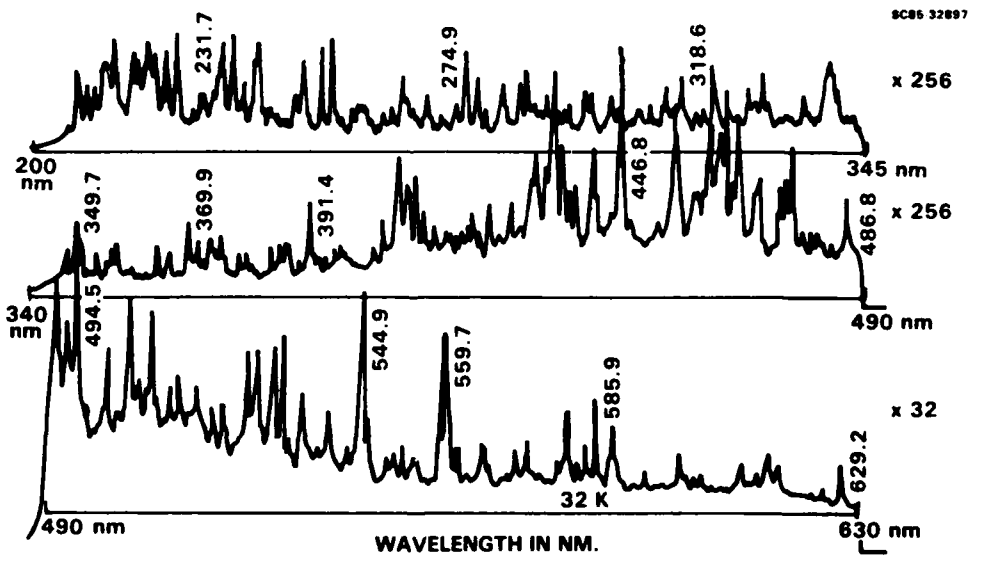

Fig. 2 Atomic emission spectrum of HfO_2 under 10.6 micron pulsed radiation. Laser fluence of 65 J/cm².

3.1.2 Atomic Species

The emission intensity, hence the density, of the excited and ionized species, increased monotonically with laser fluence but saturated at high fluence levels (> 20 J/cm^2). However, the saturation behavior depended on the ionization state with the intensity of the ground states decreasing and those of doubly ionized states increasing, but at a slower rate, with fluence. These results indicated that at high power levels, the plasma density was such that screening of the evaporation surface occurred, resulting in no net increase of the evaporated species. A larger portion of the laser energy was absorbed by the plasma, probably by inverse Bremmstrahlung, resulting in the observed shift of the populations of the ionized states towards more energetic ones. These conclusions were supported by plasma temperature data, (Fig. 3), which exhibited different dependence on fluence for low and high fluence values. This dependence became stronger for fluences higher than that where saturation of emission was observed. The plasma is directly and more efficiently heated by the laser radiation once it is dense enough to absorb this radiation.

3.1.3 Molecular Species

In these studies, molecular lines were observed in vacuum only for Al_2O_3 targets. In general, these were very weak in comparison to atomic lines. Their intensity, (Al-O, Si-O), increased with gas pressure in the mTorr range. Rather unexpectedly, this increase was observed not only in the presence of O_2 but also with such inert gases as He, Ar, and N_2. Lower emission intensities were observed in the presence of He as compared to the emission in the presence of heavier gas species (i.e., N_2). This dependence on atomic mass suggests that collisions with background atoms play a role, probably by facilitating chemical reaction (as a third body to carry away the momentum) or by cooling the plasma and retarding its expansion.

3.1.4 Ion Velocities

A time of flight method was used to determine the ionic velocities. These were in the 10^6 to 10^7 cm/s range, or 1 to 2 orders of magnitude higher than the median velocity expected from an evaporating substance under equilibrium. The velocities of the species depended weakly on fluence, as predicted from a model of a collisionally dominated plasma expanding in vacuum. The calculated ion kinetic energies were 300-1000 eV. These ener-

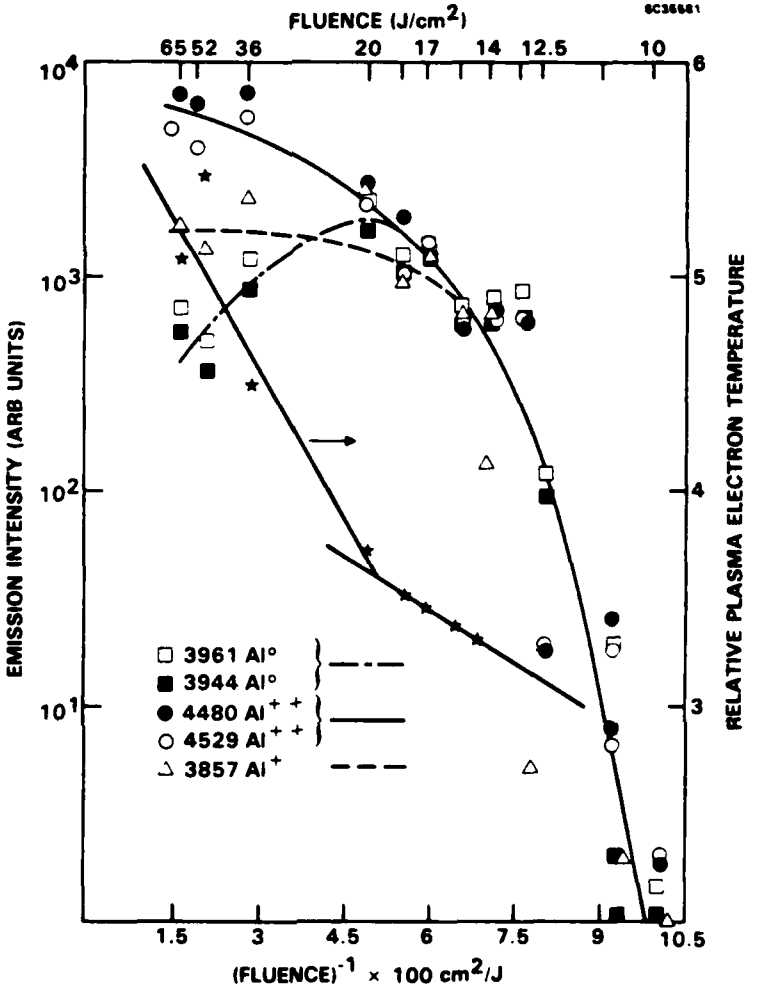

Fig. 3 Plasma temperature and atomic emission intensity vs laser fluence. Temperature was calculated from emission intensity data.

gies do not represent the plasma temperature, which was found to be in the 5-10 eV, but are a result of the hydrodynamic expansion of a hot and ionized gas into vacuum.

Most compounds and single element materials produced three different ion current velocities with one high velocity and two lower velocity components. Because elemental sources exhibited this behavior, the high and low velocity ion peaks are thought to be generated during the peak and tail portions of the laser pulse respectively, and were not attributed to ions with different atomic masses. In fact, when the tail portion of the laser

pulse was eliminated, only the high velocity ion peak was observed. Ion velocity data, obtained from different oxides with widely varying cationic masses, indicated that there was no clear dependence on atomic mass. The above observations indicate that all chemical species reach the same asymptotic velocity, independent of their mass and ionization states, because collisions in the dense plasma equilibrate the velocities.

The ion current increased monotonically with fluence.

3.1.5 Thin Film Studies

ZrO_2 thin films were deposited on room temperature glass and NaCl substrates using pulsed laser evaporation of sintered ZrO_2 ceramic targets. These films were crystalline (monoclinic) and oriented in the 100 plane. TEM analysis showed that the grain size increased with fluence (ion content) of the evaporant plume.

ZrO_2 films had refractive index values of 2.15, characteristic of bulk density ZrO_2, whereas cw laser evaporated films on room temperature substrates had index values of 1.85-1.93. Films grown by simultaneous cw and pulsed laser evaporation had monotonically increasing index values with increasing relative pulsed laser evaporation rate.

PbF_2 films were deposited by cw and pulsed laser evaporation. The crystallinity of these films increased with laser fluence. The refractive index did not depend on fluence but absorptivity increased with laser fluence. The absorptivity is attributed to preferential sputtering of F atoms from the surface.

3.2 Current Results

3.2.1 Particulates

Generation of particulates is one of the main drawbacks of the laser-assisted deposition technique. While particulates are observed in other evaporative techniques (resistive heating and e-beam evaporation), these can usually be virtually eliminated by such procedures as degassing of the source, use of baffles and wire meshes, and judicious control of power input to the sources. In pulsed laser evaporation, the generation of vapor containing energetic species, which is desired, is often accompanied by ejection of macroscopic particles. The evaporation rate and generation of energetic particles are very strong functions of power density. It was observed that particulates were invariably

generated at power densities that were necessary for evaporation with a practical rate (0.1 < r < 10 Å/s) and for minimum ion current densities for improved film properties. In the extreme case of very low power densities where particulates were not ejected, either the evaporation rate was too low to be of practical use, or insufficient energetic species were generated resulting in films comparable to those obtained using thermal evaporation. This coupling of production of particulates and energetic particles made the determination of fluence "windows" for minimum particulate density, reasonable deposition rate, and film quality, at best difficult to achieve.

The particulates that are incorporated in the film degrade film properties. While some investigators have controlled the splashing effect in easily vaporizable materials by lowering the fluence or power of the laser beam, this technique is of limited use and not applicable for refractory metal oxides.

Complete elimination of particulates for all materials by a single method has not yet been achieved. However, the use of melts as sources has resulted in virtual elimination of particulates in Ge and B_2O_3 films. Other techniques have shown considerable progress toward the same goal. Simultaneous application of more than one of these methods may result in drastic reduction or near elimination of particulates for a large class of materials.

3.2.1.1 Formation and Ejection of Particulates

Our experiments indicated that the generation of particulates and its relationship to laser conditions is material specific. Parameters such as heat of sublimation, melt viscosity, optical absorption and reflectivity, relationship of evaporation to melting temperature, thermal diffusivity, and perhaps other material parameters, affect phenomena such as dissipation of heat at the surface, advance of the evaporation front, thermal stresses and the resulting fracture of the solid. All of the above affect the size and number of particulates.

There are three possible mechanisms for the production of particulates:

- Explosive evolution of evaporant gases and ejection of loose particulates or those generated at the evaporation zone. This mechanism is especially effective if high thermal conductivity and low optical absorption cause subsurface heating of the evaporation zone;

- Melt splashing occurs when heat input to the evaporation zone is more than can be carried away by conduction, evaporative losses and radiation. The molten particles observed in the evaporation of dielectrics are ~ 10-20 μm in size and often exhibit morphological features indicative of rapid cooling;

- Partial evaporation and acceleration of particulates. These can be particulates loosely attached at the surface, probably by electrostatic charges, or those generated at the subsurface due to thermal stresses of rapid heating and cooling.

Below we discuss some of the techniques used to reduce particulate density in the films. We start with techniques used in other investigations and then give a detailed account of efforts under this program. These are summarized in Table 2.

Table 2
Techniques to Reduce Particulates

	Technique	Idea/Test	Advantages	Disadvantages
1)	Deflector vane	T	May be used for all deposition methods and materials	High rotation speeds
2)	Electrostatic Bias	T	Simple	May work in low density plasmas
3)	Colliding gas streams	T	No mechanical parts	Needs high density vapor and alignment of plumes
4)	Variable laser fluence	T	Easy to implement	Possible compromise on film properties
5)	Spinning disk source	T	Partially effective	High rotation speeds
6)	Second laser	I	Partially effective	Expense of a second high energy laser
7)	Liquid sources	T	Very effective	Limited group of materials

Techniques Used by Other Investigators

Barr developed a rotating particulate deflector vane that selectively transmitted atoms, the average speed of which is higher than that of the particulates.[16] Particulate density was significantly decreased. However, because of the distribution of particulate velocities, the particle filter still transmitted the relatively fast ones. High rotation velocities (ω = > 10000 rpm = ~ 1000 rad/s) required to operate this device in vacuum limits its reliable operation.

Greene et al.[17] reported, in the laser evaporation of Ge, that negative substrate bias of several hundred volts considerably reduced the number of particulates incorporated in the film. This effect was attributed to the electrostatic repulsion of negatively charged particulates. The particulates were assumed to be charged as spherical capacitors up to the full plasma potential due to the presence of free charges.

The latter method was used in our laboratory but failed to produce any reduction of particulate density. This was attributed to high plasma densities produced under TEA-CO_2 laser irradiation of dielectrics, and shielding of the particulates by this plasma.

Gaponov et al.,[18] used two laser beams to obtain two vapor streams that collided at an angle. The collision generated a high pressure zone that expanded in vacuum according to its own pressure gradient. The substrate was placed normal to this gradient. The particulates passed through the collision zone unaffected due to their heavy masses and missed the substrate. This technique may work if the source surfaces are continuously rendered smooth in order for the vapor streams, which propagate normal to this surface, to collide in space. Otherwise the collision zone may fluctuate in size and density due to the variation of the orientation of the vapor streams depending on morphology of the source surfaces.

3.2.1.2 Techniques Used In This Study

Our approach has been to study the nature, size and distribution of particulates, the dependence on laser and material conditions, and then to devise methods to reduce the particulate density. The particulate density was determined by counting particulates of all sizes in several representative areas of a film.

Spatial Distribution

Film thickness and particulate density were measured as a function of polar angle, the angle that the source-substrate vector makes with the normal to the source surface. Both distributions had the same angular (Fig. 4) dependence and spatially coincided with each other. Therefore, the particulate density could not be reduced by positioning of the substrate with respect to the evaporant plume alone.

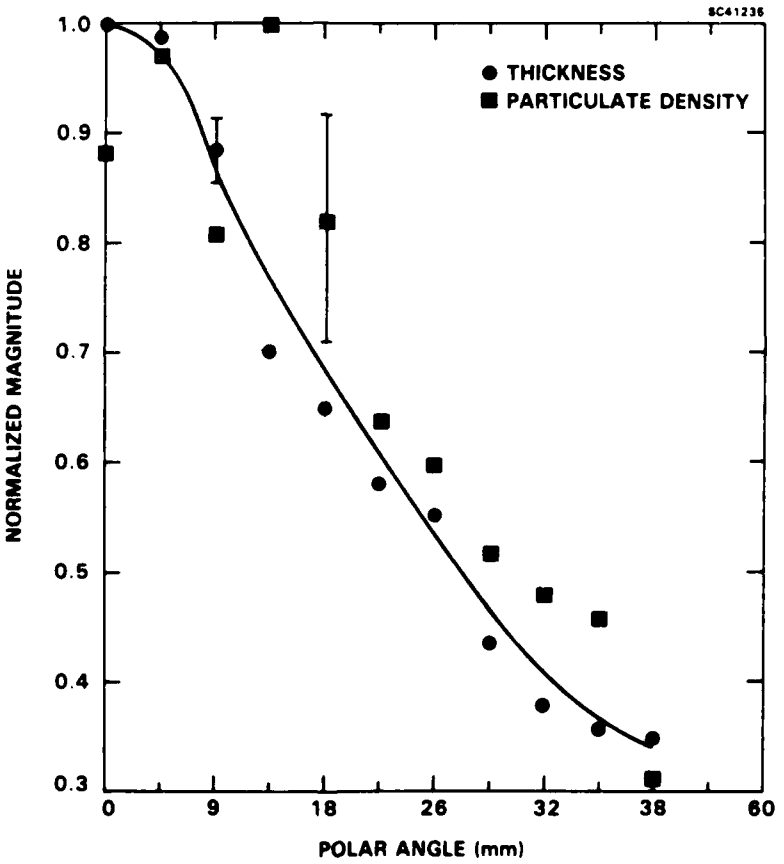

Fig. 4 Distribution of particulate density and film thickness vs polar angle from the normal to the source surface.

Material Dependence

Experiments indicated that the particulate density depends on the properties of the material such as heat of sublimation, absorptivity, the relationship of melting temperature to that of substantial evaporation, and on whether the source is solid or liquid.

In general, metal oxide dielectrics that have high absorptivity for 10.6 μm radiation produced fewer particulates than solids such as ZnS, ZnSe, NaCl, Si that are transmissive at this wavelength. This behavior of transmissive materials is due to subsurface heating because of their lower absorptivities. In some experiments plates or wafers of these materials were irradiated with high power laser and film and particulates were deposited on substrates exposed to both faces of the plate. Particulates generated at the side where the laser beam exited were larger and more numerous than those at the entry side of the plate. The higher (by a factor of n, the refractive index) field strength at the exit surface may account for this phenomenon.

The sources formed by sintering, or hot or cold pressing, powder material produced more particulates than the sources prepared by vacuum melting and solidification. The difference for Ta_2O_5 and TiO_2 films is a factor of two and three reduction, respectively, in particulates. On the other hand, annealing of sintered powder sources at temperatures as high as 1100°C before evaporation did not result in any reduction of particulate density.

Materials that have a low melting temperature relative to their evaporation temperature, taken as the temperature at which the vapor pressure is 10^{-4} Torr, tend to produce large molten droplets.

Melts as Evaporation Sources

Use of melts as evaporation sources resulted in virtual elimination of particulates in films of Ge (Fig. 5) and B_2O_3. For Ge, this was observed at all fluence levels. Several properties of the material can account for these observations. The absence of solid particulates, that might be accelerated by the vapor expansion or by jet action due to partial evaporation; highly absorptive material due to the presence of free carriers and consequent localization of heat at the melt surface; low volume of vapor due to high reflectivity of the surface and high heat of vaporization of Ge.

SC39318

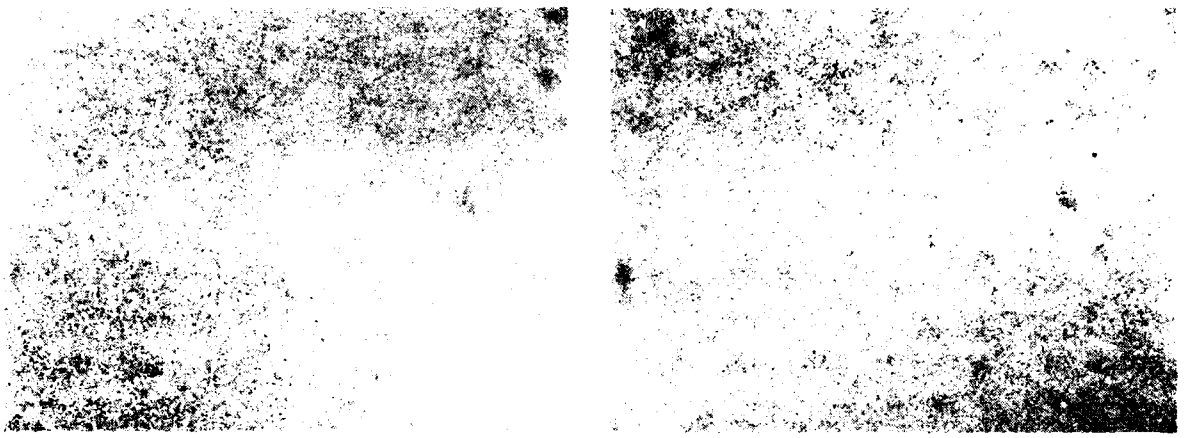

SOURCE = SOLID Ge at 700°C
THICKNESS = 650Å

(a)

SOURCE = LIQUID Ge at ~ 1000°C
THICKNESS = 1300Å

(b)

Fig. 5 Surface morphology of Ge films deposited by pulsed laser evaporation. (a) Solid source, and (b) liquid source.

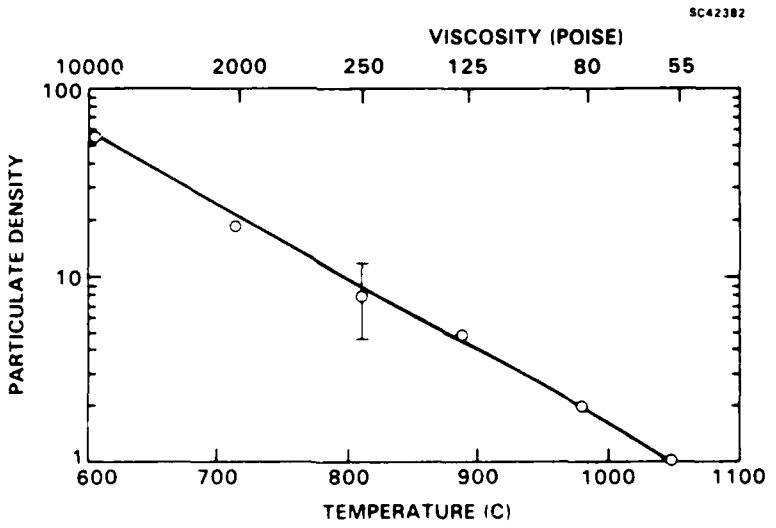

Fig. 6 Particulate density in B_2O_3 films vs B_2O_3 melt temperature. Viscosity of B_2O_3 is also indicated on the upper abscissa.

Particulate-free films of B_2O_3 could be obtained only at certain fluence levels (see next section) and for high source temperatures where the melt viscosity was low. The particulate density in B_2O_3 films was a strong function of temperature (Fig. 6).

Two properties of the melt, viscosity and thermal conductivity, depend on temperature. The effect of the latter is small: Specific heat and density do not depend on temperature[19] for B_2O_3, therefore, the increase in thermal conductivity directly affects thermal diffusivity. An increase in thermal diffusivity[19] of 60% increases the volume heated by diffusion only by 25% since the diffusion distance is given by, $\sqrt{Dt}$, where D is the diffusivity and t is time, taken to be the laser pulse width.

On the other hand, the change in viscosity upon increasing source temperature from 600 to 1100°C is roughly a factor of 200 (Fig. 6).[20] Viscosity affects the plastic yield of the material and therefore plays a major role in determining whether or not molten particulates are ejected. This also explains the difference in the behaviors of Ge and B_2O_3 melts. Ge has very low viscosity (v), typical of metals at the melting point ($v_{Ge} = 5 \times 10^{(-3)}$ poise) but B_2O_3 is still quite viscous even at the highest temperature ($v_{B2O3} = 55$ poise).

Another significant advantage of using melt sources is the invariant or self-healing source surface morphology. The alteration of surface morphology in solid sources causes several undesirable effects:

- Spreading of the beam over an area, varying with the local morphology, affects the evaporation rate. The latter has exponential dependence on fluence, (energy/area), because of the exponential dependence of the vapor pressure on temperature.

- The evaporant stream is normal to the local surface and changes direction depending on surface morphology. These problems are eliminated when liquid sources are used.

The technique of using liquid sources for laser evaporation, although very successful, is applicable to a limited group of materials. Substances that have stable melts with low vapor pressure and without decomposition are metals, Ge and some dielectrics such as Ta_2O_5, TiO_2. Many useful materials sublime or form a very thin molten layer at the surface during evaporation, and therefore are not suited for this method.

Laser Fluence Dependence

Since generation and acceleration of particulates are phenomena of thermal origin, the laser fluence or the energy density was expected to play a major role in the particulate problem. The particulate density was found to strongly depend on laser fluencewith a nonmonotonic behavior.

At very low fluences (< 10 J/cm^2) characterized by the evaporation threshold, the particulate density is low. As the fluence increases, so does the particulate density. Apparently, surface heat is sufficient to fracture the material and partially vaporize and accelerate the particulates. These are solid particulates, often with jagged morphology. At higher fluences, very low solid particulate density is obtained, probably because of complete evaporation of the surface layer.

At the highest fluences (> 100 J/cm^2) large spherical droplets appear in the film, probably by solidification of melt ejecta. Spherical droplet density is one or two orders of magnitude lower than that of solid particulates. A deep melt is formed on the source surface in this regime, which does not vaporize completely, and is the source of the observed molten droplets via mechanisms discussed above.

Similiar behavior is observed in the fluence dependence of molten droplets originating from a melt (Fig. 7). Particulate density is very low at low fluence levels. As fluence increases, the number of particulates rapidly increases and then gradually decreases. Very low particulate density is achieved at the highest fluences again, an observation that suggests complete vaporization of the surface layer or any ejected mass in its transit through the laser beam.

There are two regimes of operation from a practical point of view. Either very low fluence levels must be used, sacrificing rates of evaporation and generation of energetic species, or highest fluence levels can be used, and the presence of some particulates must be tolerated.

Spinning Source Disks

Another approach is the use of a source in the shape of a disk rotating at high speeds (Fig. 8). This causes separation of particulates from the atoms. This separation is based on the difference in their velocities (v_p and v_a) normal to the source surface, men-

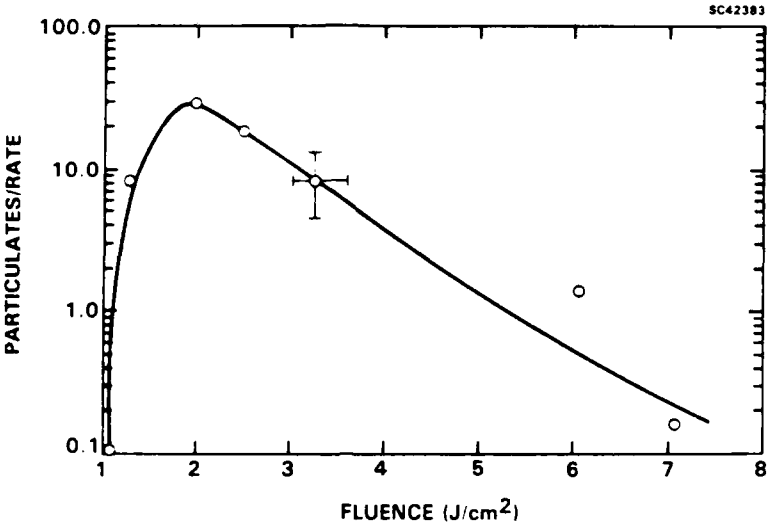

Fig. 7 Ratio of particulate density to the rate of thin film deposition vs laser fluence in pulsed laser evaporation of B_2O_3 melts.

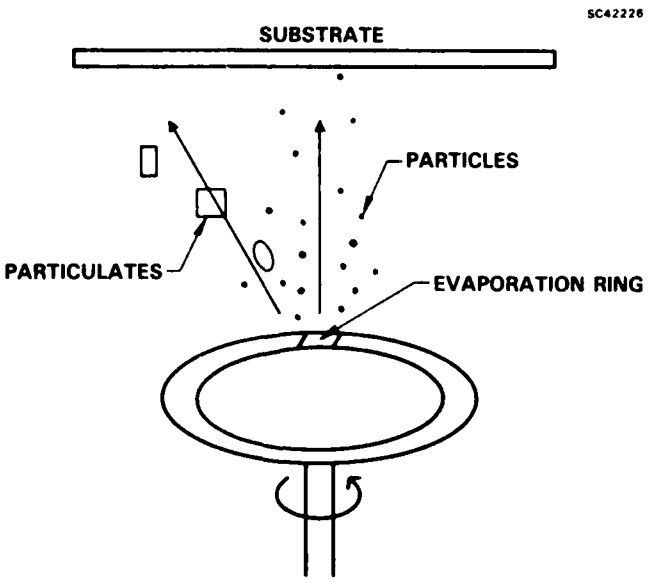

Fig. 8 Schematic of rotating laser evaporation source.

tioned earlier. If the periphery of the disk is used for evaporation, all or most particles and particulates will have the same tangential velocity v_t when they leave the disk surface. However, since $v_a >> v_p$, the particulates will drift in the tangential direction for a longer period of time. Thus, particulate density will shift with respect to the film thickness distribution and substrates placed away from the peak of particulate distribution will have fewer particulates.

Experiments confirmed that the particulate density on one side of a large (7.5 cm diameter) substrate was lower than on the other side (in the direction of the tangential velocity). This difference was a factor of 2 for disk rotation speeds of ~ 10000 rpm and source-substrate distances of 15 cm. Since this method spatially separates the particle and particulate distributions, the effectiveness can be increased by increasing the source-substrate distance. This method is simpler to implement than the deflector vane wheel mentioned above because of the smaller rotational inertia of a small disk. However, high speed rotation in vacuum environment is still required. Also, because particulates emanate with a wide angular distribution and have a wide spread in their normal velocities, the technique reduces but does not eliminate the problem.

Use of a Second Laser Beam

The use of a second laser beam to "burn" the particulates in their flight was conceived as a method to reduce the particulate density. This second laser beam must be synchronized but delayed with respect to the first beam that causes the evaporation because the evaporation and ejection of particulates do not start until after the peak of the evaporating laser pulse. This long delay time makes optical time delay impractical. Electronic delay between two lasers can be used.

A first order analysis indicated that the size (a_o) of the particulates that can be completely vaporized is related to the laser and material parameters as follows

$$a_o = E(1 - R)\ U/s^2$$

where

E = laser energy/pulse
R = reflectivity of the surface

s = beam size
U = specific heat of sublimation

Incomplete vaporization will also reduce the number of particulates incident on the substrate since these particulates will be accelerated away from the source-substrate axis by the jet action of the escaping vapor. Analysis indicated that the particulate size (a) is related to the material parameters and angle of deflection from this axis by the following:

$$a = a_o \left[1 - \exp(-v/v_g \tan \alpha)^{-1}\right] \approx a_o \frac{v_a}{v \tan \alpha}$$

where

v = normal velocity of the particulates
v_g = vapor velocity

Assuming laser energy of 1 J, and that all of the nonreflected energy is converted into heat, the size of the particulates that can be completely evaporated is $a_o \sim 10$ μm, and those that can be deflected at an angle of 45 is $a \approx 100$ μm for typical materials.

The variation of the time of arrival of the particulates (ms) to the waist of the second beam, in relation to the pulse duration, which is microseconds, will make it impossible for all of the particulates to be evaporated.

Among various approaches that have been considered, adjustment of the laser power and careful preparation of the source material are the most practical and generally applicable ones.

3.3 Thin Film Studies

3.3.1 IR Optical Thin Films, Ge

Ge Films

Thin films of Ge deposited by thermal and by laser evaporation of molten sources were analyzed. Films deposited by pulsed laser evaporation on crystalline substrates were found to be much more crystalline and oriented than their thermal counterparts (Fig. 9). Experiments clarified the role of energetic ions on the nucleation and densification of films.

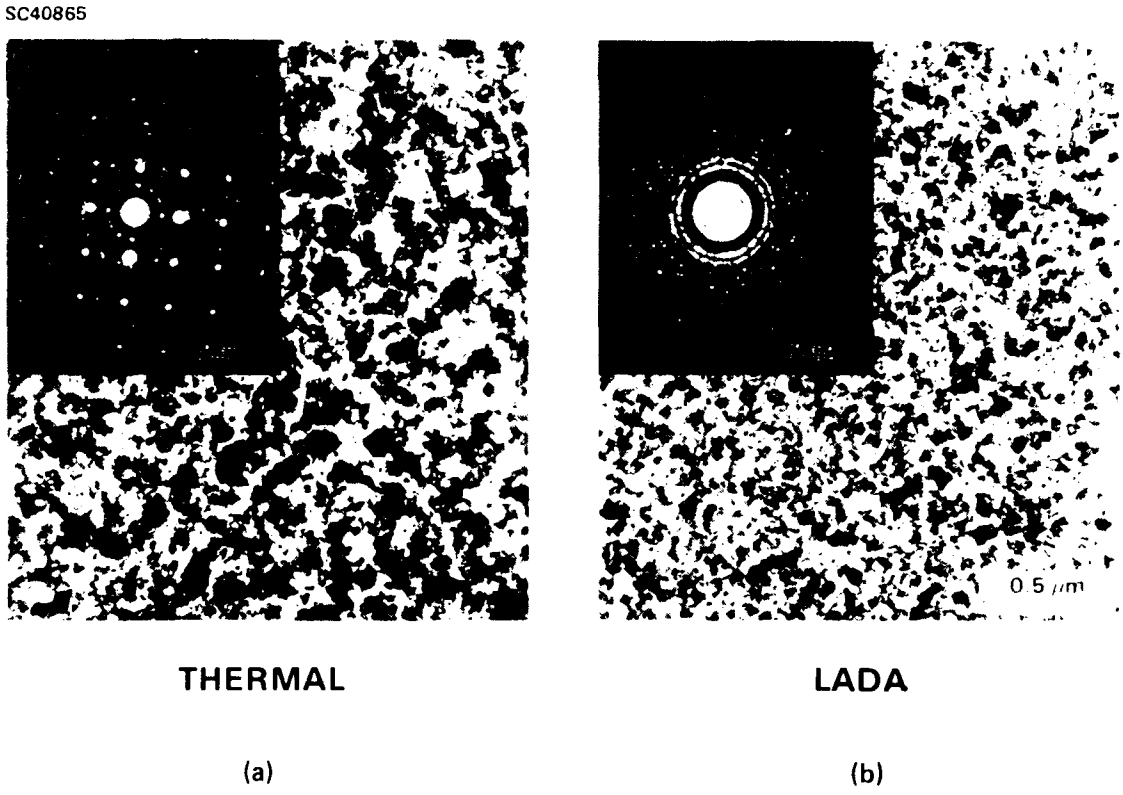

Fig. 9 Transmission electron micrographs of Ge films; (a) deposited by pulsed laser evaporation of Ge melts, and (b) deposited by thermal evaporation.

3.3.1.1 Structural Properties, Epitaxial Films

Germanium films deposited on NaCl and Si substrates at 300°C were single crystal (Fig. 9) and oriented in the 100 direction when deposited by pulsed laser evaporation, and polycrystalline, with considerably smaller grain size, when deposited by thermal evaporation. Microstructure was studied using TEM analysis of the films grown on NaCl chips, and x-ray diffraction and electron channeling (Fig. 10) analysis of the films grown on Si. It is to be noted that no special cleaning procedure was used for Si except for degreasing with organic solvents. Elaborate cleaning methods and ultrahigh vacuum are generally used for epitaxial growth of Ge on Si at similar or higher temperatures. These results suggest that similar careful surface preparation techniques might result in even lower epitaxial temperatures.

Films deposited at lower substrate temperatures were polycrystalline, with those prepared by laser evaporation exhibiting a higher degree of orientation and larger grain size than the thermal films.

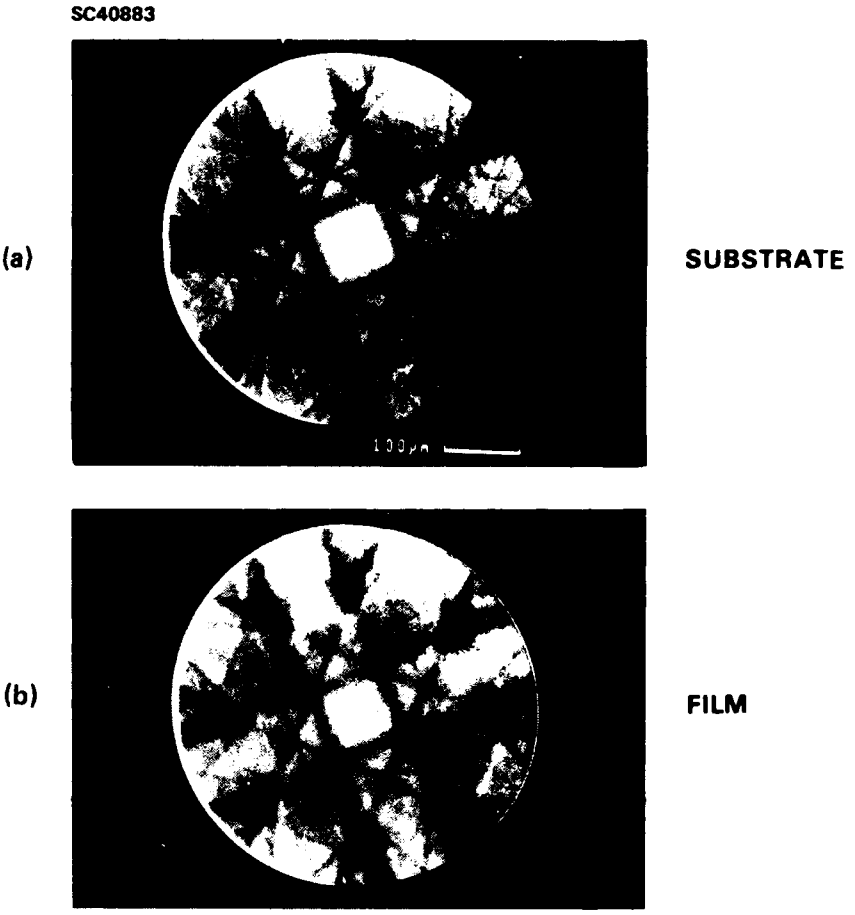

Fig. 10 Electron channeling diffraction patterns of Ge films deposited by pulsed laser evaporation on Si substrates. (a) Thin film, and (b) Si substrate.

The crystalline and morphologically smooth Ge films can be used as substrates for GaAs or CdTe films. Thus, epitaxial GaAs or CdTe films on Si substrates with the intermediate Ge films can be used to make monolithic devices that have optoelectronic and signal processing capability.

3.3.1.2 Role of the Ions in the Nucleation and Densification

To understand the role of the laser-generated energetic species on thin film properties, films were grown according to the designs of Table 3. Comparison of structural properties indicated that (c) was single crystal and (a) was slightly more crystalline than (b). Sample (d) exhibited the least amount of structural order. These results suggest that

energetic particles in the vapor stream play a more important role in nucleation than in the subsequent phases of film growth. In other words, once numerous oriented crystalline nuclei form due to the effects of energetic particles on the substrate surface, crystalline order can be maintained by deposition using less energetic thermal evaporation.

Table 3
Laser Evaporation From Ge Melts

	Deposition Sequence	TEM Pattern
a)	100Å (Laser) + 900Å (Thermal)	Rings with dots
b)	100Å (Thermal) + 900Å (Laser)	Rings with diffused dots
c)	1000Å (Laser)	Dots
d)	1000Å (Thermal)	Rings

3.3.1.3 Morphology

Films deposited by laser-assisted evaporation had very smooth and featureless morphology whereas the thermally evaporated film had the typical rough morphology reported in the literature (Fig. 11).[21] The enhanced surface adatom mobility under energetic ion bombardment that promotes layer-by-layer growth can account for these results.

3.3.1.4 Properties of the Ions

The ionized part of the Ge evaporant stream was characterized by means of a translatable Faraday cup. The ion current exhibited three distinct peaks with velocities of 5.5×10^6 cm/s, and 2 and 2.4×10^6 cm/s, for the fast and slow ions, respectively. The low velocity ion peaks, that in an earlier study were found to be due to the tail portion of the laser peak, were more prominent for liquid than solid Ge sources (Fig. 12). A possible explanation is the increased absorptivity of molten Ge due to the presence of free carriers. If a linear proportionality between free carrier absorption and carrier density were to hold into the liquid state, the absorptivity at these wavelengths would be 4×10^5 cm^{-1}. This high absorptivity makes it possible for the lower power density tail to generate its own plasma and resulting energetic species. The tail portion of the laser pulse does not generate a dense plasma from solid Ge, which has considerably lower absorptivity.

SC40884

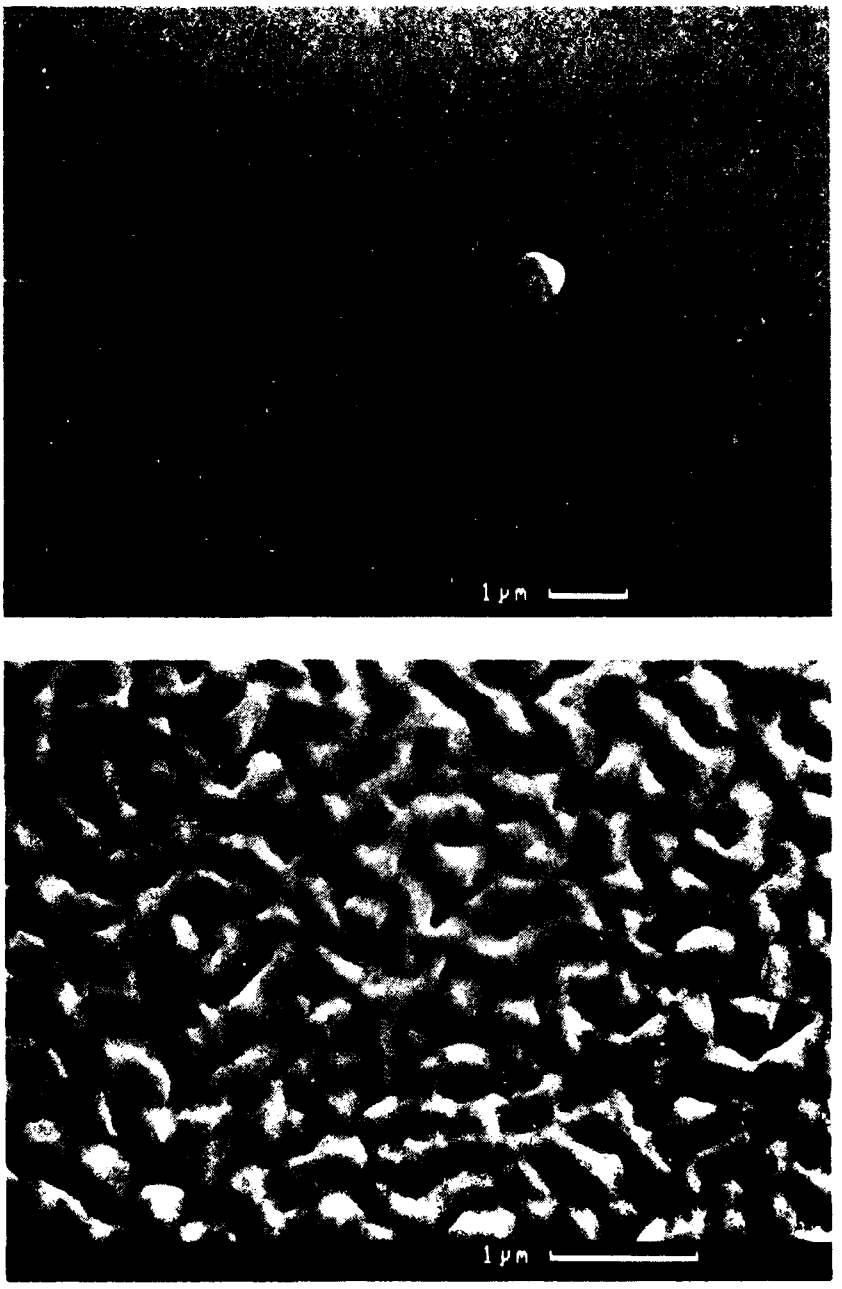

Fig. 11 Surface morphology of Ge films deposited on Si substrates at 300°C. (a) Thermal evaporation, and (b) pulsed laser evaporation.

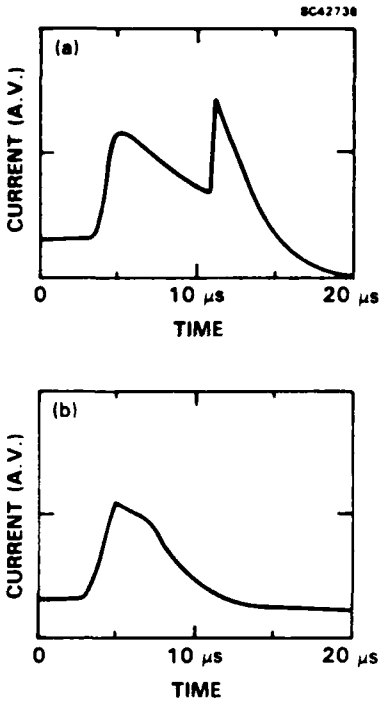

Fig. 12

Ion flux vs time in the pulsed laser evaporation of Ge. (a) Liquid Ge source, and (b) solid Ge source.

3.3.2 Visible Wavelength Optical Thin Films

Pulsed laser evaporated thin films of refractory metal oxide dielectrics, such as TiO_2, HfO_2 and Ta_2O_5, were studied. Refractive index values were higher than can be obtained by e-beam evaporation alone. However, higher absorptivities were also observed. Some films had crystalline structural order even when deposited at room temperature. A novel reactive deposition technique was successfully demonstrated for TiO_2 films resulting in the highest refractive index values yet observed (n = 2.44) for room temperature deposited films.

3.3.2.1 TiO_2 Films

Films deposited on room temperature glass and NaCl substrates exhibited significant crystalline order. The former were analyzed by x-ray diffraction and the latter by TEM. In contrast, thin films deposited by e-beam evaporation on substrates at 300°C did not exhibit any evidence of crystallinity. The crystalline phases were Ti suboxides, Ti_5O_9 or Ti_9O_{17}. Paucity of diffraction lines prevented unambiguous identification of the dominant phase. TEM analysis indicated that the crystallites were small (200Å average size) were dispersed in an amorphous matrix. These crystalline films were obtained only at the highest laser fluences (~ 120 J/cm^2).

Optical Properties

The refractive index (n) of the films deposited at room temperature was 2.3-2.35, and at 300°C was 2.35-2.41. These values are higher than can be obtained by e-beam evaporation on unheated substrates (n = 1.95-2), or on heated (T = 200°C) substrates (n = 2.1-2.15). These films had high absorptivity (k = 0.01-0.05) whereas the e-beam deposited films had one or two orders of magnitude lower extinction coefficients. Annealing in air lowered the extinction coefficients by about one order of magnitude, but did not change the structural properties.

Particulates

TiO_2 films deposited by pulsed laser evaporation of an e-beam melted source did not exhibit any reduction of particulate density over that obtained using sintered pellets. Since the vapor pressure of liquid TiO_2 is high, source temperature could not be increased to form a deep melt; instead only a thin skin of melt was formed by the e-beam in these experiments. This condition and other material parameters (e.g., melt viscosity) could account for these observations.

Laser-Induced Plasma Reactive Evaporation

TiO_2 films were deposited by pulsed laser evaporation in a plasma activated medium with the goal of reducing the absorptivity of the as-grown films (Fig. 13). The plasma was formed only briefly within the laser-generated plasma plume from the source material. This plasma plume, expanding between two electrodes biased at 400 V, initiated plasma breakdown in the background O_2 gas at 10^{-4} Torr pressure. No hot electrodes, that have short lives in highly oxidizing ambients, were used. Rather, a cold cathode discharge, that ordinarily requires high pressures > 10^{-3} Torr, was obtained at relatively low pressures due to the presence of the conducting volume of gas between the electrodes. These films had the highest refractive index values for TiO_2 obtained by evaporative techniques, (n = 2.44). However, the absorptivity did not change, suggesting that energetic ion bombardment and preferential sputtering of oxygen are still very effective in controlling the oxidation of Ti and its suboxides, even in the presence of active oxygen.

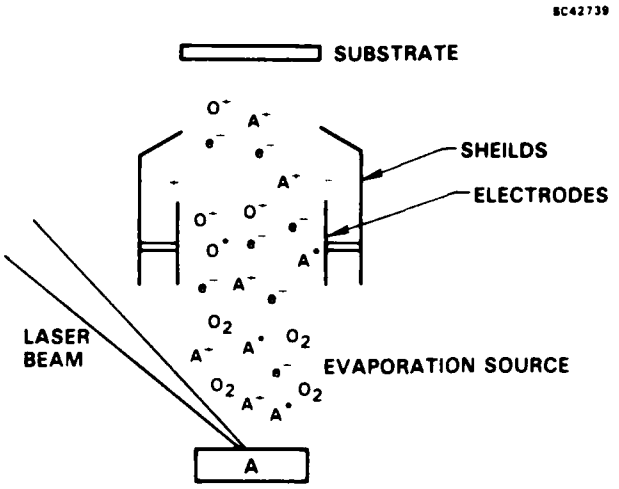

Fig. 13

Schematic of apparatus for laser activated plasma reactive evaporation.

3.3.2.2 HfO_2 Films

HfO_2 films exhibited all the advantages and none of the drawbacks of pulsed laser evaporation. Films had a very high refractive index (n = 2.152). The refractive index of e-beam evaporated films on heated substrates is 1.95, increasing to 2.0 after 300°C annealing. Laser-evaporated films had smooth morphology with no particulates, and were not absorbing indicating complete oxidation of the metal. Oxidation is affected by surface reaction kinetics and by the degree of preferential sputtering of oxygen. Since sputtering or momentum transfer between colliding bodies passes through a maximum when the masses are equal, the different behavior of Ti, Zr and Hf oxides can be explained partially on the basis of their atomic weights. The atomic weights increase in the order of O, Ti, Zr, Hf and the corresponding oxides have decreasing absorption, as grown, in that order.

HfO_2 films were composed of oriented grains with monoclinic and orthorhombic structure. Crystallinity (grain size and orientation) was a strong function of laser fluence.

3.3.2.3 Ta_2O_5

Tantalum pentoxide films, deposited by pulsed laser evaporation, were completely amorphous but had a high refractive index (n = 2.05). This could be obtained at power density levels that produced relatively few submicron size particles, the density of which was $1.5 \times 10^4/cm^2$. The absorptivity of these films was comparable to those grown by e-beam evaporation.

3.3.2.4 CeO_2 Films

Films grown from CeO_2 sources were crystalline and dense. These films were oriented and had a high degree of structural order as indicated by x-ray diffraction analysis. Films grown under high fluences (~ 100 J/cm^2) had the Ce_6O_{11} structure and those grown at lower fluences (25 J/cm^2) were CeO_2. All films were grown under identical conditions of substrate temperature, gas pressure, and deposition rates. Therefore, it is thought that loss of O_2 due to preferential sputtering at high fluences may produce suboxides.

The refractive index of the films deposited at room temperature was 2.42 and the extinction coefficient was in the range of 0.001-0.01.

3.3.2.5 Diamond-Like Carbon Films

Thin films of carbon were deposited by pulsed laser evaporation of high purity graphite on Si and quartz substrates. These films had very smooth morphologies and a mostly amorphous structure. Selected area diffraction results indicated that small (~ 50Å) grains of possibly crystalline material are embedded in the amorphous structure. Raman spectra of the film clearly indicated that the film was a mixture of graphitic and diamond-like material (Fig. 14). Two peaks can be resolved in this spectrum that correspond to different modes of C-C vibrations.

Electrical resistivity of the diamond-like carbon films increased with laser fluence. The highest resistivity was 600 Ω-cm. This is 2×10^4 times higher than the resistivity of graphitic films obtained by cw laser evaporation of graphite.

Optical properties also depended on laser power. Transmission properties of the best quality film is shown in Fig. 15 and compared to films obtained by cw laser evaporation of graphite and diamond.[22] The refractive index values were 2.2-2.6 for 1.06 wavelength. The absorption in the visible range was high (1000 cm^{-1}) and depended strongly on wavelength. IR absorption of the best films was between 400 and 500 cm^{-1} for the wavelength range of 2-10 microns.

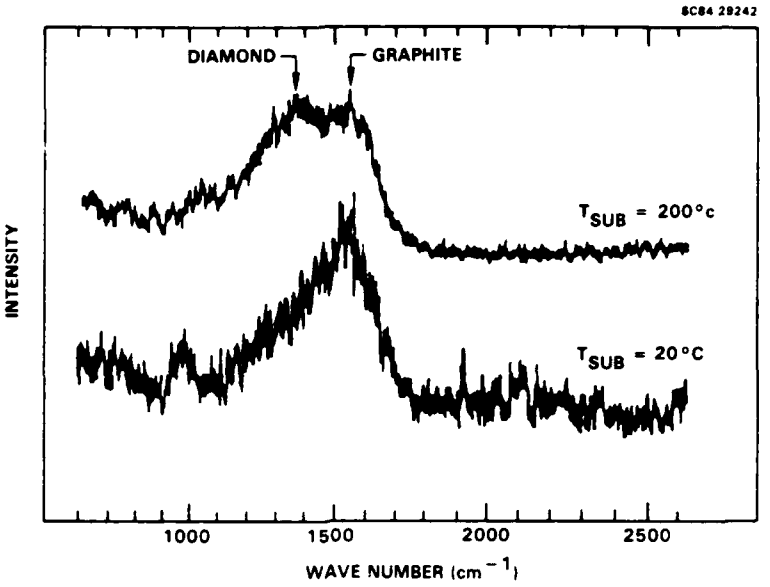

Fig. 14 Raman spectrum of diamond-like carbon films deposited by pulsed laser evaporation of graphite targets. Laser fluence was 125 J/cm^2.

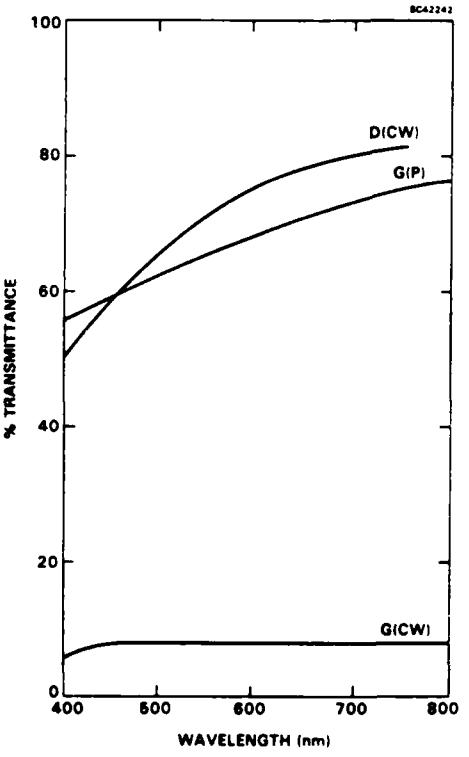

Fig. 15

Visible wavelength transmission spectrum of the best diamond-like carbon film deposited by pulsed laser evaporation of graphite (GP). For comparison, films deposited by cw laser evaporation of diamond (DC) and graphite (GC) from Ref. 22 are shown. All films are 1000Å thick.

Optical analysis of the plasma emission indicated neutral, singly, doubly and triply ionized species. The emission intensity, or number density, increased with fluence, and saturated for fluence values above 20 J/cm^2. Electrical analysis of the plume indicated 5 distinct ion arrival times or ion velocities. These ranged from 2-10 $\times$ 10^6 cm/s. These velocities were not numerical multiples of each other. This suggests that a possible simple model of an accelerating potential is not valid, since this would require that species in different ionization states have velocities that are multiples of each other. No molecular species (i.e., C-C,C-O) were observed.

4.0 CONCLUSIONS

Pulsed laser evaporation has recently become a practical and feasible technique for thin film deposition. It offers several advantages over other physical vapor deposition techniques. Congruent evaporation is important in preserving the film and source stoichiometry of, especially, multicomponent materials. Recent success with the deposition of high T_c superconducting materials[6] is a good example. The presence of highly energetic, as well as ionized and excited species in the vapor has been shown to improve density and microstructure of the films as well as the corresponding macroscopic properties. Several limitations have also been identified. The rate of evaporation, density, and energy of energetic species are coupled through their dependence on laser power, and therefore lacks the elements of control of competing ion-assisted deposition techniques. Even though similar degrees of improvement of film properties can be achieved by both techniques, this limitation may restrict the range of usefulness of laser evaporation. On the other hand, laser-assisted evaporation is a high vacuum technique. The bombarding ions are the same species as those that constitute the film. Therefore, entrapment of gases (e.g., Ar) and the resulting degradation of film properties is eliminated in this technique. Splashing or generation of melt drops or solid particulates imposes limitations on deposition conditions and usable materials. However, it is expected that future developments in this area will alleviate this problem. Below we discuss some of the practical aspects of this technique.

4.1 Practical Aspects of Pulsed Laser Evaporation

In the practical application of this technique the quality of the films, the rate of evaporation, uniformity over large area substrates and compatibility with other concurrent deposition techniques must be considered.

Rate of Evaporation

Laser evaporation rates are limited by the power input to the laser source, heat of sublimation, surface reflectivity and heat losses. The power output of typical TEA-CO_2 lasers is ~ 30 W, that of excimer and Nd:YAG lasers is ~ 10 W. Taking into account the losses in the optical elements used to deliver a focussed beam onto the sources (e.g, 15% in

molybdenum mirrors), source reflectivity (e.g., ~ 21% in TiO_2), and nonevaporative processes, the deposition rate for typical materials is calculated to be ~ 5-10Å/s. These values are calculated with the additional restriction of uniform deposition over a substrate 3 cm in diameter. The observed rate is often less, indicating that a smaller fraction of the beam energy goes into vapor formation. Some of the possible energy loss paths are: (a) the energy in the periphery of the laser beam heats the source but not to the point of vaporization; (b) absorption and reflection of the energy by the plasma, and (c) pressure of the vapor displaces the melt, thus removing it from the evaporation zone. The heat of fusion of the displaced material will not contribute to the evaporation.

The above arguments indicate that high rates of evaporation (> 5Å/s) over large substrates cannot be obtained due to power limitations of typical laboratory lasers.

Laser Fluence

Many of the advantages of the pulsed laser evaporation are realized only when highest fluences are used, especially for dielectric materials. Furthermore, medium rates (1-5Å/s) and for some materials even low rates (0-1Å/s) of evaporation can be obtained only at these high fluences. As mentioned in Section 3.2.1, particulates are generated at these fluences. Often a compromise between film crystallinity, rate and particulate density must be made.

5.0 REFERENCES

1. Smith, H.M., Turner, A.F., Applied Optics 4, 147 (1965).

2. Stephen, A.W., Zrebiec, T.J., Ban. V.S., Mater. Res. Bull. 9, 1427 (1974).

3. Cheung, J.T., Magee, T., Vac. Sci. Tech. A1, 1604 (1983).

4. Lynds, L., Woody, B.A., J. Elec. Spect. Rel. Phenom. 29, 147 (1983).

5. Sankur, H., Denatale, J., Gunning, W., Nelson, J., J. Vac. Sci. Tech. A5, 2869 (1987).

6. Dijkkamp, D., Venkatesan, T., Wu, X.D., Shaheen, S.A, Jisrawi, N., Min-Lee, Y.H., McLean, W.L., Croft, M., Appl. Phys. Lett. 51, 619 (1987).

7. Cheung, J.T., Madden, J., J. Vac. Sci. Tech. B5, 705, 1987.

8. Cheung, J.T. to be published in Appl. Phys. Lett.. Dec 1987.

9. Sankur, H., Woodbury, F., Hall, R.H., Gunning, W., Mat. Res. Symp. Proceed. 77, 727, (1986)

10. Schwartz, G.P., Bondybey, V.E., English, J.H., Gualtieri, G.J., Appl. Phys. Lett. 42, 952 (1983).

11. Krokhin, Laser Handbook, edited by Arecchi, F.T., Dubois, E.O., North Holland, 1371-1407, 1972.

12. Ready, J.F., J. Appl. Phys. 36, 462 (1965).

13. Caruso, A., Gratton, R., Plasma Physics 10, 67 (1968).

14. Hughes, T.P., Chapters 7 & 8, Plasmas and Laser Light, J. Wiley and Sons, 1975.

15. Martin, P.J., J. Mater. Sci. 21, 1 (1983).

16. Barr, W.P., J. Phys. E. 2, 1024 (1969).

17. Lubben, D., Barnett, S.A., Suzuki, K., Gorbatkin, S., Greene, J.E., J. Vac. Sci. Tech. B3, 968 (1985).

18. Gaponov, S.V., Gudkov, A.A., Freerman, A.A., Sov. Phys. Tech. Phys. 27, 1130, (1982).

19. Thermophysical Properties of Matter, v_2 and v_5, Y.S. Touloukian, editor, Plenum Press (1972).

20. Sperry, L.L., Mackenzie, J.D., Physics and Chemistry of Glasses 9, 91 (1968).

21. Ohmachi, Y., Nishioka, T., Shinoda, Y., J. Appl. Phys. 54, 5466 (1983).

22. Fujimori, S., Kasai, T., Inamura, T., Thin Solid Films 92, 71 (1982).

List of Publications

H. Sankur, Properties of thin PbF_2 films deposited by cw and pulsed laser-assisted evaporation, Applied Optics, 25,1962 (1986).

H. Sankur, J.G. Nelson, A.T. Pritt, Jr., W.J. Gunning, Plasma luminescence generated in laser evaporation of dielectrics, J. Vac. Sci. Tech. A5, 15 (1987).

H. Sankur, J. DeNatale, W.J. Gunning, J.G. Nelson, Dense crystalline ZrO_2 thin films deposited by pulsed laser evaporation, J. Vac. Sci. Tech. A5, 2869 (1987).

H. Sankur, W.J. Gunning, J. DeNatale, Low temperature epitaxial Ge films deposited by pulsed laser evaporation, to be sent to Appl. Phys. Lett.

H. Sankur, J.T. Cheung, W.J. Gunning, Deposition of dielectric thin films by pulsed laser evaporation, to be sent to J. Phys. as invited paper.

Conference Presentations

H. Sankur, W.J. Gunning, J. DeNatale, Deposition of ZrO_2 thin films by pulsed laser evaporation, Mater. Res. Sympos, Anaheim, CA, April, 1987.

H. Sankur, J.G. Nelson, A.T. Pritt, Jr., Plasma luminescence generated in laser evaporation of dielectrics, Optic. Soc. Meet., Baltimore, Oct, 1985.

H. Sankur, Properties of PbF_2 thin films deposited by laser evaporation, Optic. Soc. Meet., Baltimore, Oct, 1985.

H. Sankur, W.J. Gunning, Deposition of dielectric thin films by pulsed laser-assisted evaporation, to be presented in OSA topical meeting on thin films in Tucson, AZ, April 1988.

6.0 APPENDICES

6.1 Properties of thin PbF_2 films deposited by cw and pulsed laser assisted evaporation

H. Sankur

Properties of thin PbF_2 films deposited by cw and pulsed laser assisted evaporation

Haluk Sankur

Thin films of lead fluoride were deposited by means of cw or pulsed laser assisted evaporation and were characterized for their structural and optical properties. Continuous wave laser evaporated films had smooth morphology, good optical transmission, and oriented columnar grain structure. The crystallinity of the pulse laser evaporated films, as measured by x-ray diffraction peak intensities, was found to be higher than the cw laser or e^--beam evaporated films and was found to depend on the laser pulse energy density (fluence). These films, however, had higher absorption in the visible range.

I. Introduction

The performance, stability, and even feasibility of many optical devices depend on the physical properties of the thin films that constitute these devices. Physical vapor deposited films are well known to contain voids, the fraction of which can be as large as 40% for some evaporated materials (e.g., CaF_2).[1] The effect of this is a lower than bulk and somewhat process-dependent refractive-index, ambient sensitivity due to adsorption of moisture that alters the values of the index and thin film stress. Several novel approaches (e.g., ion assisted deposition)[2] that address the above problem have been successfully tried. These techniques enhance the adatom mobility by depositing controlled amounts of energy at the growth surface.

The technique used in our study, laser assisted evaporation, is a high-vacuum physical vapor deposition technique where the average energy of the evaporating species is higher than thermal energy. Some advantages of these techniques are (a) congruent evaporation of most compounds; (b) high-kinetic-energy content of the vapor in the plume[3]; (c) existence of ionized and excited species in the plume[4]; (d) complete dissociation of the molecular species.[5] Therefore, the laser becomes a heat source to vaporize as well as impart hyperthermal energies to a fraction of the evaporants. In (b) and (c) the energy transport to the surface is in the form of kinetic and electronic energy of the atoms, whereas in (d) molecular heat of dissociation is released at the surface.

PbF_2, an intermediate index (1.76), soft material, useful for the visible and IR range (0.25–17-μm transmission range), was chosen to study the characteristics of the evaporation processes. Thin PbF_2 films deposited by cw and pulsed CO_2 lasers as well as by e-beam evaporation were characterized to understand the effects of the laser evaporation conditions on the structure and optical properties of the films. It was found that the structural order can be enhanced using a high-power pulsed laser. The increased crystallinity of the films is attributed to the high-energy content of the evaporant plume and possibly to the pulsed nature of the evaporation.

II. Experimental

Details of the experimental apparatus for the laser evaporation are described in Ref. 6. The source material was a mixture of α- and β-PbF_2 in pellet form. The films were grown on glass and low-conductivity Si substrates at room temperature and at pressures of 2×10^{-7} Torr. The average deposition rate was 20 Å/s, and film thickness was 1 μm. To study the effect of the rate of deposition on the film properties the rate was varied in the 0.1–100-Å/s range. Similarly the effect of ambient gases was studied by varying the O_2 pressure in the system in the 2×10^{-7}–5×10^{-5}-Torr range. Oxygen was chosen to also investigate the possibility of formation of lead oxides or oxyfluorides.

The cw CO_2 laser was used unfocused, whereas the pulsed laser (a Lumonics model 820 CO_2 TEA laser, 3-J maximum pulse energy) was focused to various spot sizes by AR-coated ZnSe lenses. The pulsed laser output was varied between 0.125 and 0.4 J, whereas the fluence was varied between 0.1 and 30 J/cm^2 by varying

The author is with Rockwell International Center, P.O. Box 1085, Thousand Oaks, California 91360.

Received 8 February 1986.
0003-6935/86/121962-04$02.00/0.

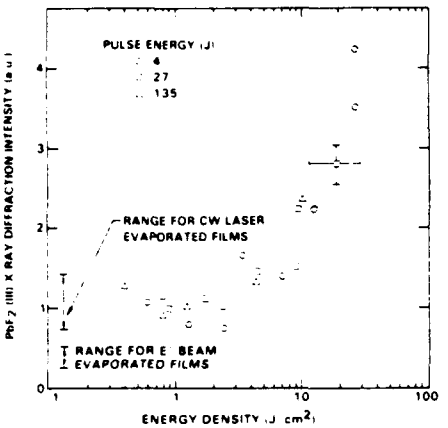

Fig. 1. Crystallinity of PbF_2 films vs laser beam energy density.

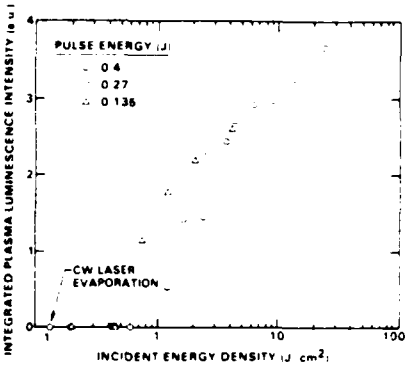

Fig. 2. Plasma luminescence intensity vs laser beam energy density.

both the focused spot size and incident energy. The focused spot size was determined by measuring the dimensions of burn patterns on ground glass or Styrofoam slabs.

The films were analyzed by x-ray diffraction for structural properties. The optical parameters, index and extinction coefficient were obtained by analyzing the transmittance and reflectance spectra of the films in the 0.4–0.8-μm range and curve fitting by varying the dispersion parameters. The curve fitting method that uses a converging power series in a chromatic coordinate is explained in Ref. 7.

The luminescence in the evaporant plume due to laser-matter interaction was analyzed by means of an optical multichannel analyzer coupled to a spectrometer in the 200–900-nm range. The pressure variations due to pulsed evaporation were measured by means of an ionization gauge. The contents of the evaporation plume were investigated by an RGA. Both the ion gauge and RGA were in direct line of sight to the source.

A. Continuous Wave Laser Evaporation

Continuous wave laser evaporated films were found to have smooth morphology and columnar grains as observed under SEM analysis. The refractive index (1.76 at 632.8 nm) was found to be independent of evaporation rate from 0.1 to 100 Å/s. The films were oriented in the ⟨111⟩ direction with minute amounts of ⟨311⟩ orientation of β-phase. Films thicker than 5 μm showed evidence of cracking. The optical properties of the films were similar to the films prepared by e-beam evaporation, although the latter had less structural order (Fig. 1). The films prepared by boat evaporation (ceramic coated tungsten wire boats) had poor crystallinity and high absorption. No evidence of excited species luminescence was observed in the plume of the cw laser evaporated material. Comparison of the plume contents by a quadrupole mass analyzer failed to indicate any consistent difference between PbF_2 evaporated from a boat and by a cw laser. In each case F_2, F, Pb, PbF, PbF_2, and Pb^+ signals were observed. Visual inspection of the source material did not indicate decomposition in the case of cw laser evaporation; extensive decomposition occurred in the thermal evaporation boat.

B. Pulsed Evaporation

The temporal nature of the evaporation under pulsed laser irradiation was determined with an ionization gauge located above the source. The pulsed laser produced pressure rises of up to 10^{-4} Torr from a base pressure of 2×10^{-7} Torr. The time constant of the electronics of the ionization gauge apparatus did not allow accurate measure of the decay time of the pressure spike and may also have limited the measure of the height of the spike; however, assuming the evaporation times comparable to laser pulse width (approximately microseconds) and using calculated deposited thickness per pulse (0.1–2 Å/pulse), very high ($\geq 10^5$ Å/s) instantaneous rates can be expected to occur during pulsed laser deposition. The average deposition rate was maintained at 20 Å/s by adjusting the pulse repetition rate (10–50 Hz) for each energy density level.

The x-ray diffraction intensity of the (111) β-PbF_2 line of the films grown by pulsed laser evaporation and other techniques is shown in Fig. 1. The crystalline order, interpreted as the degree of orientation of the grains and the order within the grains, shows a steep increase for laser pulsed fluences above 1-J/cm^2 threshold. Below this threshold the effect on crystallinity of the deposition method whether pulsed, cw laser or e-beam, was minimal.

The threshold for increased crystallinity also coincided with the onset of luminescence from the plume (Fig. 2). Detailed analysis of the luminescence indicated many atomic lines that belong to Pb and F neutral and ionized states (Fig. 3). The luminescence intensity of Fig. 2 is the integrated signal over the spectral range of response of a photodiode. This signal consists of a continuum background and many well-defined sharp emission lines. The laser power dependence of the individual emission lines intensities, which are representative of the number density of the emitting species, was in general different from the dependence shown in Fig. 2. The latter consisted of a

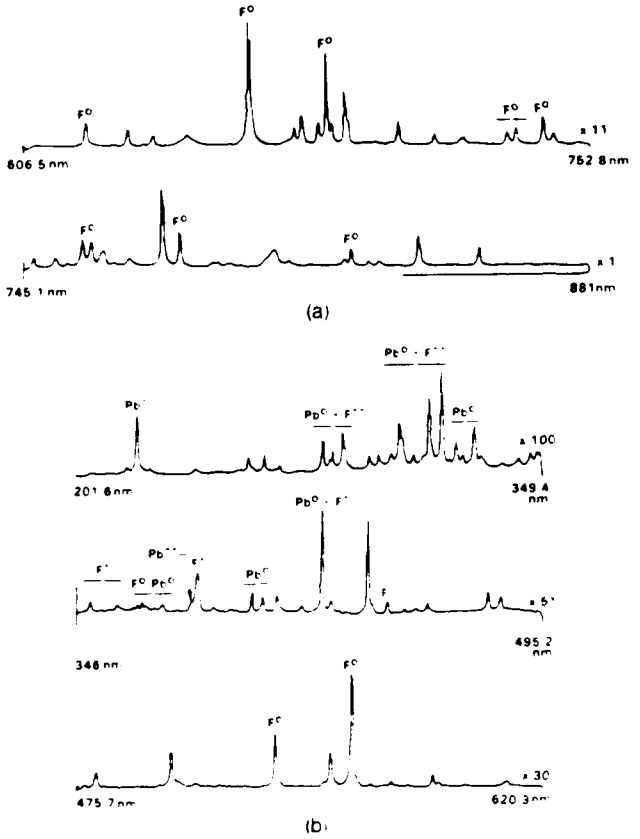

Fig. 3. Luminescence spectra of PbF_2 by CO_2 TEA laser heating (power density ~5 × 10^7 W cm^{-2}). (a) 201.6–620.9 nm range; (b) 606.5–881 nm range. Note the scale factors for each spectrum.

threshold followed by steep increase with beam energy density and saturation beyond 20 J/cm^2.

The refractive index of the films was found to be 1.76 ± 0.02, independent of growth conditions. The extinction coefficient, however, showed a clear dependence on the incident energy density with the films grown at higher fluences being more absorptive (Fig. 4). These films were also found to have particulates (0.1–1-μm size) in the form of jagged chunks similar to those in the source pellet and for the highest fluences in the form of rounded disks indicative of splashed molten droplets. The source material was observed to be discolored and to contain minuscule metallic particles reminiscent of the boat evaporated source material, which also became severely discolored and decomposed to produce millimeter size Pb beads.

SEM observation indicated that the films had columnar grains. TEM analysis confirmed the crystal symmetry of the structure and did not indicate any free Pb clusters that were expected to account for the absorption. Analytical techniques based on e-beam excitation of the material, such as Auger analysis, were found to decompose the surface of PbF_2 and thus did not provide reliable stoichiometric data. Possible stoichiometric differences between the cw and pulsed laser grown films were found to be beyond the sensitivity of XPS analysis (~1%). XPS analysis did not indicate free or oxidized states of Pb.

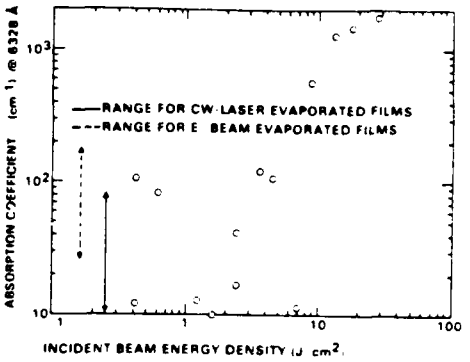

Fig. 4. Absorption coefficient at 632.8 nm of PbF_2 films vs laser beam energy density.

III. Discussion

The structure and optical properties of evaporated thin PbF_2 films were found to depend on evaporation conditions. The effect of the pulsed laser assisted evaporation on the thin film structure is believed to be due to the presence of energetic species (i.e., ions, excited species, and particles with high kinetic energies) and possibly to the UV radiation in the evaporant plume. The effect of these is presumably increased surface adatom mobility and rearrangement.

The effect of very high instantaneous deposition rates, where the energy of formation and sublimation of PbF_2 are released at the surface in a very short time, must also be considered as a possible rapid annealing heat source. Assuming that the deposition takes place during the laser pulse time t_p and that the heat is released within the diffusion distance ($\sqrt{D \times t_p}$, where D is the heat diffusivity of the material), instantaneous temperature excursions of 250°C are calculated for 1-Å/pulse average PbF_2 deposition rate. These temperature excursions are high enough that some annealing of the growing layer could occur.

Future planned experiments that will investigate the relative abundance and the role of the ions (e.g., by electrostatic deflection or retardation) and the effect of the high deposition rates (that can be varied with the source to substrate distance) should clarify the above issue.

Small amounts of free Pb was observed in the source material following evaporation by pulsed laser or by joule heating of a crucible due to decomposition of PbF_2. This suggests that the absorption in the films grown under these conditions may be due to excess Pb incorporated in the films by coevaporation of Pb with PbF_2. Since the vapor pressure of Pb over PbF_2 is higher than that over Pb,[8] high local temperatures (e.g., near the crucible walls or at the center of the pulsed laser beam) are necessary to coevaporate Pb with PbF_2.

The possibility of high deposition rates contributing to optical absorption must be considered, because under these conditions free Pb may be buried in the film

before it has reacted with fluorine. In the pulsed laser evaporation, less than a monolayer (~1 Å) is deposited per pulse followed by a 20–100-ms interval where the surface is bombarded by residual fluorine and background gases, thus giving Pb ample exposure for reaction. Thus it is concluded that the evaporation rather than deposition conditions account for the high absorption in the films deposited by pulsed laser or joule heating.

IV. Conclusion

The properties of PbF_2 films grown by cw and pulsed CO_2 laser assisted evaporation have been analyzed and related to growth conditions. Continuous wave laser evaporation produced morphologically smooth and oriented films that are transparent in the visible and IR. The properties did not depend on the deposition rate or background pressure.

The films grown by pulsed laser evaporation were found to have a higher degree of crystallinity, which was directly dependent on the pulse energy density (fluence). Since the emission intensity of the excited species in the evaporant plume also scales with laser fluence, the increased crystallinity is assumed to be due to the effect of the energetic particles in the plume promoting increased surface adatom mobility. These films were also found to have higher optical extinction coefficients.

The author gratefully acknowledges W. Gunning and J. T. Nelson for many useful discussions, E. H. Cirlin for SEM analysis, P. Kobrin for XPS analysis and revision of the text and the partial support of AFOSR under AFOSR #F49620-84-C-0091.

References

1. H. K. Pulker, "Characterization of Optical Thin Films," Appl. Opt. **18**, 1969 (1979).
2. P. J. Martin, R. P. Netterfield, and W. G. Sainty, "Modification of the Optical and Structural Properties of Dielectric ZrO_2 Films by Ion Assisted Deposition," J. Appl. Phys. **55**, 235 (1984).
3. e.g., L. Lynds and B. A. Woody, "Nonequilibrium Behavior on Pulsed Laser Evaporated Surfaces," J. Electron Spectrosc. Relat. Phenom. **29**, 147 (1983).
4. H. Sankur, J. Nelson, and C. A. Pritt, "Emission Luminescence Analysis of Pulsed Laser Evaporated Plume," to be published in J. Vac. Sci. Tech.
5. J. T. Cheung, "Mechanism of Laser Assisted Evaporation of II-VI Compounds," Mater. Res. Soc. Symp. Proc. **29**, 301 (1984).
6. H. Sankur and J. T. Cheung, "Highly Oriented ZnO Films Grown by Laser Assisted Evaporation," J. Vac. Sci. Technol. **A1**, 1806 (1983).
7. W. H. Southwell, "Determining Index Dispersion of Thin Films," J. Opt. Soc. Am. A **1**, 1279 (1984).
8. e.g., Data in O. Kubashewski, E. L. Evans, and C. B. Alcock, *Metallurgical Thermochemistry* (Pergamon, New York, 1979).

6.2 Plasma luminescence generated in laser evaporation of dielectrics

H. Sankur, J.G. Nelson, A.T. Pritt, Jr., and W.J. Gunning

Plasma luminescence generated in laser evaporation of dielectrics

H. Sankur, J. G. Nelson, A. T. Pritt, Jr., and W. J. Gunning
Rockwell International Science Center, Thousand Oaks, California 91360

(Received 21 February 1986; accepted 28 September 1986)

Emission from the plasma generated when a pulsed CO_2 laser is used to evaporate dielectric materials is analyzed in the 200–900 nm region by means of an optical multichannel analyzer. Atomic spectra consisting of excited neutral and singly, doubly, and triply ionized species were observed from laser irradiation of Al_2O_3, SiO_2, ZnO, PbI_2, TiO_2, and HfO_2. Emission from the B–X transition of AlO was observed under vacuum conditions becoming more intense in the presence of added gases. Assuming local thermal equilibrium, plasma temperatures were calculated using the emission intensities of several selected atomic species. Possible effects of the observed phenomena on the properties of thin films deposited by laser-assisted deposition are discussed.

I. INTRODUCTION

Many of the properties of thin films depend on the structure of the film. In the case of optical thin films, the packing density, crystalline order, and orientation affect the optical (e.g., index) and mechanical (stress) properties as well as ambient sensitivity of these films. Similarly, electrical characteristics are sensitive to the structural order in the case of semiconductor films.

The structure depends not only on the material and substrate temperature, but also on the deposition process.[1] It has long been recognized that deposition of evaporated species allows limited degree of control on the film structure, especially when the substrate temperatures are kept below optimum growth temperatures.[2] Several novel deposition methods (e.g., ion-assisted deposition) that utilize nonthermal means of raising the effective surface temperature and enhancing surface adatom mobility have produced dense crystalline structure in thin films. Pulsed laser-assisted deposition is one such emerging technique which has a unique combination of advantageous features and has been used to produce high-quality films for electro-optical applications.[3] It produces congruent evaporation of compounds with near complete dissociation of molecular species.[4] In addition, the evaporant plume contains ions and excited species.[4] The latter are thought to impart hyperthermal energies to the film growth surface and improve structural properties by enhancing surface adatom mobility.

Since the advent of high-power lasers, many aspects of the interaction of the laser radiation with materials have been studied. These studies include laser damage in laser transparent materials,[5] laser radiation–matter interactions at very high power densities used for fusion related work,[6] and laser-induced breakdown in absorbing materials in air.[7] However, detailed analyses of the laser-vaporized and excited plume used in the thin-film deposition process and study of the relationship of energetic plume constituents and film properties have not been made. This work addresses the first issue by employing optical techniques to analyze the plume.

A high-power (3 J/pulse) CO_2–TEA laser was used to vaporize various dielectric targets (e.g., Al_2O_3). The resulting plume was analyzed with an optical multichannel analyzer. Numerous excited neutral and singly, doubly, and some triply ionized species were identified. In addition, by using a local thermal equilibrium model, the temperature of the plasma was calculated using the intensity of selected atomic lines. Finally, the dependence of the luminescence intensity on both laser power and ambient gas pressure was studied.

II. EXPERIMENTAL

The luminescence experiments were performed in a stainless-steel vacuum chamber (Fig. 1) in which the base pressure was maintained in the 2×10^{-8} to 2×10^{-7} Torr range. The chamber was fitted with NaCl windows that are transmissive to 10.6-μm laser radiation as well as ultraviolet (UV) and visible radiation from the plume luminescence. A Lumonics (model 810) TEA–CO_2 laser was used in multimode operation. The CO_2 laser beam was focused on the targets using 40-cm focal length NaCl or Ar-coated ZnSe

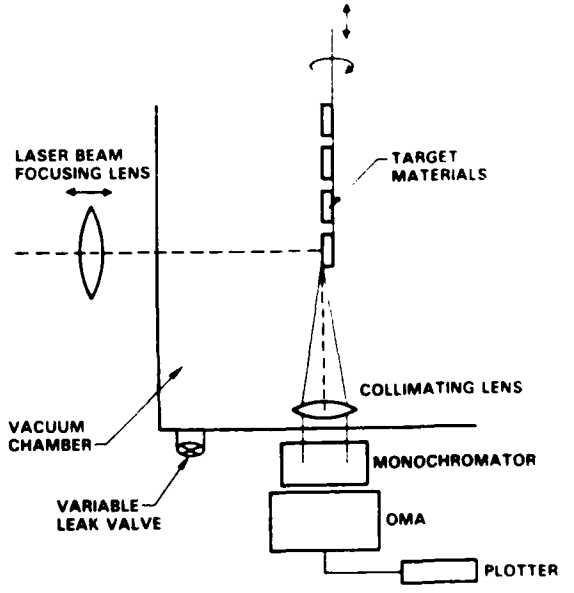

FIG. 1. Schematic of the experimental apparatus used in the luminescence studies.

 0734-2101/87/010015-07$01.00

lenses, the position of which with respect to the target could be varied in order to vary the power density on the target. The laser power was also attenuated using Fresnel reflection plates of ZnSe, NaCl, GaAs, and Ge, which when used in various combinations provided incremental attenuation in 5% steps. The method of varying the discharge voltage to vary the laser output was not used, except in one experiment, since this also alters the divergence and the mode distribution in the beam. The laser pulse consisted of a main peak that was 100 ns wide followed by a smaller tail which ended at ~ 1 μs. The fraction of the energy in the tail could be adjusted by varying the laser gas mix.

Laser pulse energy was measured with a Gentec model ED 500 energy meter. The maximum laser output of 3 J was reduced to ~ 2 J at the target due to attenuation in the molybdenum mirrors used to steer the beam on the target and Fresnel losses in windows and lenses. The amount of energy actually absorbed by the target was less than the above value due to reflectivity of the targets. The average reflectivities are given in Table I. The incident energy densities were varied from 3 to 65 J/cm^2 by the above-mentioned methods.

The targets consisted of crystalline sapphire, fused quartz, and sintered pellets of ZnO, PbF_2, HfO_2, and TiO_2. The positions of these with respect to the laser beam were varied to expose fresh surface or new material (Fig. 1).

The chamber pressure was maintained at $\sim 2 \times 10^{-7}$ Torr during most of the experiments. In the experiments to study the effect of the ambient gases on the plasma luminescence and the feasibility of reactive evaporation, a leak valve was used to introduce gases, the pressures of which were controlled between 2×10^{-5}–2×10^{-1} Torr. These gases were ultrahigh purity grade N_2, O_2, Ar, and He.

The plasma luminescence was observed at right angles to the laser beam path. The emissions were dispersed by an $f/3$ Jarrel–Ash 0.25-m monochromator fitted with a 600 line/mm holographic grating. The dispersed radiation was detected by a focal plane array consisting of 1024 25-μm-wide detecting elements. A Tracor Northern (model 1710) optical multichannel analyzer used to store and sum individual spectra. With this combination of grating and camera, spectral intervals of 190-nm bandwidth were collected. A low-pressure Hg discharge lamp was used to calibrate the spectrum from 200–900 nm. The resolution of the monochromator (25-μm slits) and OMA was ~ 2 Å per element. A slight nonlinearity in the dispersion grating affected absolute wavelength accuracy so that even when both ends of the OMA scan were calibrated by a Hg lamp, the center region was found to deviate by as much as 5 Å. Since the plasma luminescence was intense, it was not necessary to focus the emitted light onto the monochromator slit. On occasion, neutral density filters were needed to prevent saturation of the detector array.

TABLE I. Reflectivity (R) values for the materials studied at 10.6 μm (Ref. 8).

Material	R
Al_2O_3	0.16
SiO_2	0.15
TiO_2	0.21
PbF_2	0.32
ZnO	0.20

III. RESULTS

A. Luminescence

The typical temporal behavior of the plasma emission is shown in Fig. 2. This example is of a Si^0 line at 440 nm and is also characteristic of other lines. The decay time of the luminescence is ~ 1 μs, which correlates with the laser pulse width including the tail. The spectrum of Al_2O_3 from 200–900 nm is shown in Figs. 3(a) and 3(b). Only the prominent peaks are labeled, but most of the 222 lines seen in this spectral range were identified[9] as either neutrals, or singly, doubly, or triply ionized atomic species. Molecular species were observed only for Al_2O_3 under high-vacuum conditions. The SiO_2 spectrum contained a significant number of identifiable lines. The spacing of the lines in the Al_2O_3 and SiO_2 spectra was sufficiently large that the lines could be unambiguously assigned. Such was not the case for HfO_2 and TiO_2. The extremely rich emission spectrum of Hf and Ti resulted in overlap of many features which made assignment of the lines very difficult. Identification of spectral lines was further complicated by the slight nonlinearity of the wavelength axis of the OMA. Hence, only the Al_2O_3 and SiO_2 spectra were used for quantitative analysis.

The spectra of ZnO and PbF_2 could also be unambiguously analyzed. These contained many neutral and singly ionized lines, but relatively few doubly ionized atomic emission lines. The apparent lower excitation level in the plume can be attributed in part to lower laser absorptivities and in part to higher vapor pressures (P) for these materials relative to those of the other four oxides. The laser energy is absorbed in a larger volume yet substantial evaporation occurs at relatively low temperatures (e.g., $P = 10^{-4}$ Torr at < 820 °C for PbF_2).

The intensity of each of the atomic lines is directly proportional to the number density of the emitting state. The relative emitting state distribution, therefore, can be obtained by dividing each atomic line intensity by its associated spontaneous emission rate[10] weighed by its degeneracy. A plot of the log of the excited state distribution for atomic aluminum versus their respective state energies is presented in Fig. 4. Except for the point designated as 3961 Å in Fig. 4, these data indicate a linear relationship in which the slope determined by a linear least-squares analysis defines a Boltzmann temperature of 6600 K. Although the number of emitting states presented in Fig. 4 is not extensive, the state distribution strongly suggests that local thermodynamic equilibrium is established within the viewing volume of the spectrometer.[11]

Each of the atomic transitions reported in Fig. 4 terminates on the ground state, placing a major caveat in this analysis. If a significant population of ground-state atoms is present in the plume, radiation trapping of these atomic transitions alters the analysis. The oscillator strengths for these transitions, however, are similar and the change in the

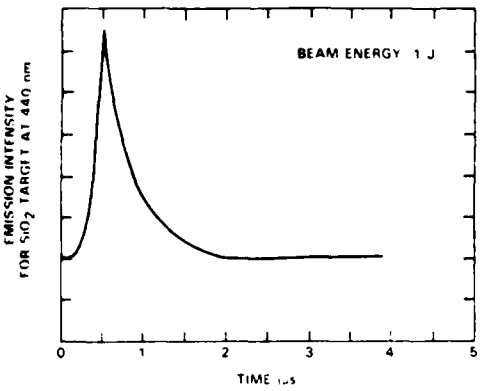

FIG. 2. Temporal behavior of the luminescence signal of the evaporant plume of SiO_2 at 440-nm wavelength.

effective emission rate due to trapping results in similar lifetime lengthening for each of the emitting states. If the degree of trapping is relatively small, these systematic errors would tend to cancel, leaving the interpretation of the results unaltered.

A similar analysis for the excited states of silicon neutrals is presented graphically in Fig. 5. For the silicon emissions, the Boltzmann temperature (6700 K) is of the same order of magnitude as that found for Al. Both Al_2O_3 and SiO_2 are not transmitting at 10.6 μm, have similar reflectivities (see Table I) and similar bond energies. Hence, it is not surprising that the atomic state distributions for neutral Al and Si atoms yield similar temperatures when subjected to equivalent laser fluxes.

B. Power and pulse-shape dependence

The power density dependence of the plasma emission was studied by varying the incident laser energy density by using attenuators and lenses in the path of the beam. Figure 6 shows the intensity versus reciprocal laser energy of neutral (3961, 3944 Å), singly ionized (3587 Å) and doubly ionized (4525, 4480 Å) Al species. At low energy levels, all species emit at roughly the same intensity. But, as the power is increased, the neutral species intensity passes through a maximum at 20 J/cm^2 and then decrease in intensity. The doubly ionized species continue to increase in intensity past the 20

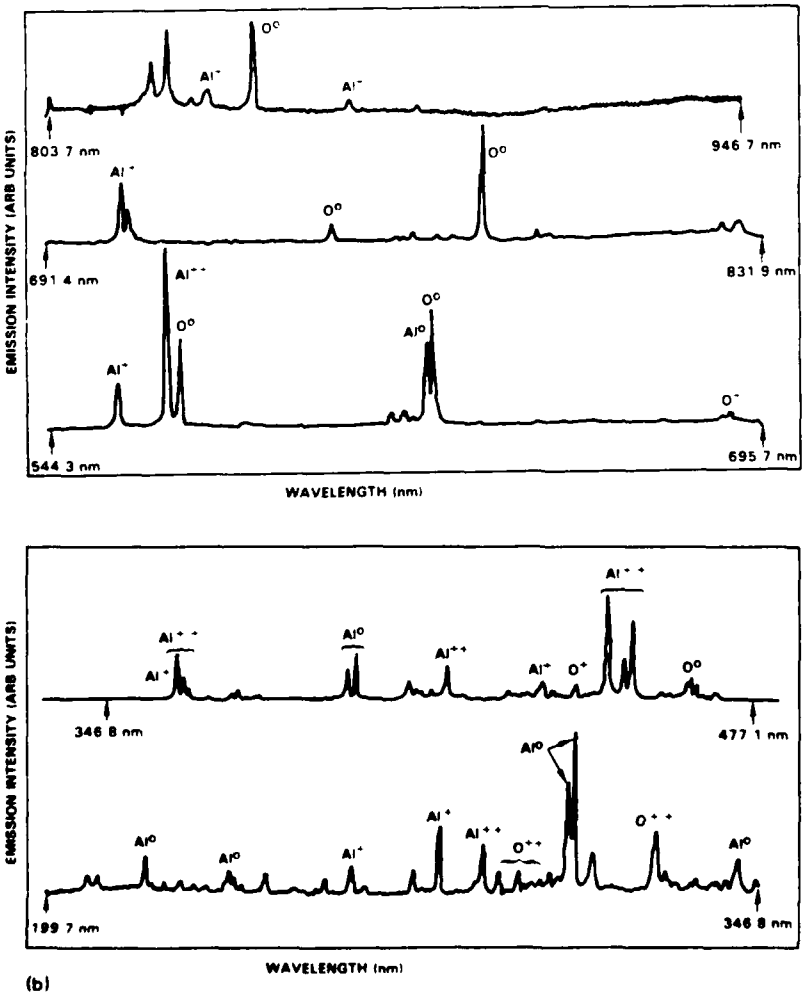

FIG. 3. Spectrum of the luminescence of the evaporant plume of Al_2O_3 under TEA–CO_2 laser radiation. (Power density $> 10^8$ W/cm^2.)

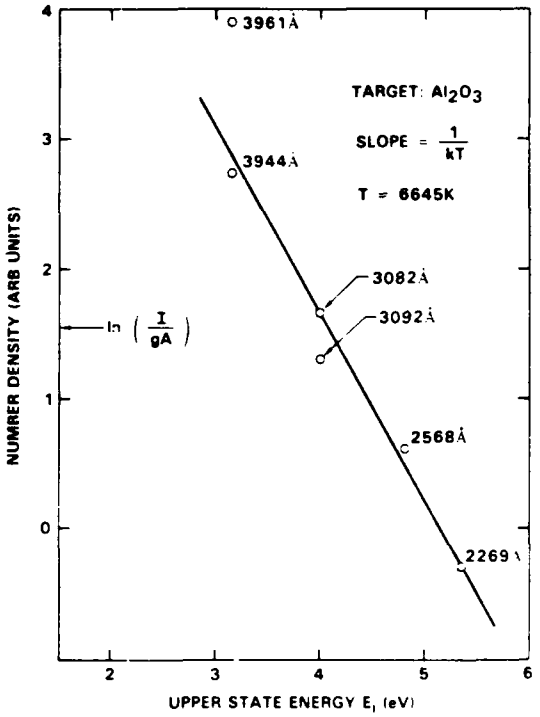

FIG. 4. Number density of the Al luminescent species plotted vs initial excited state energies in the evaporant plume of Al_2O_3 (20 J/cm^2).

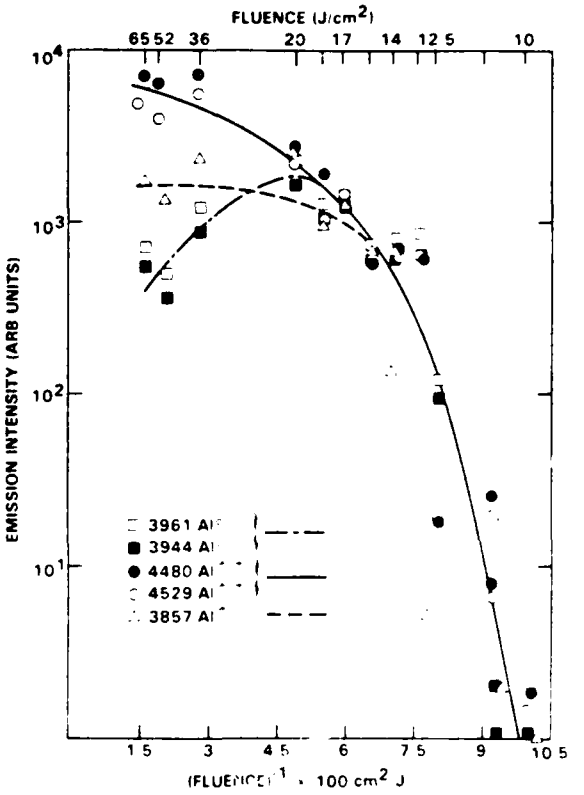

FIG. 6. Incident laser energy dependence of selected neutral and ionized emission line intensities in the evaporant plume of Al_2O_3.

J/cm^2 fluence point, however, with a weaker dependence on fluence. The case of singly ionized species is in between the behavior of neutral and doubly ionized species.

The above-described behavior at high fluences can be attributed to the absorption of the incident laser radiation by the plasma. As the laser energy increases, the plasma becomes more dense as additional material is vaporized. After reaching a critical density, the absorption of the laser radiation in the plasma increases so that the latter becomes opaque to the laser.[12] This absorbed energy goes into creating more highly ionized species, thus increasing the Al^{++} and Al^{+} emission over that of the neutral species. Figure 7 shows

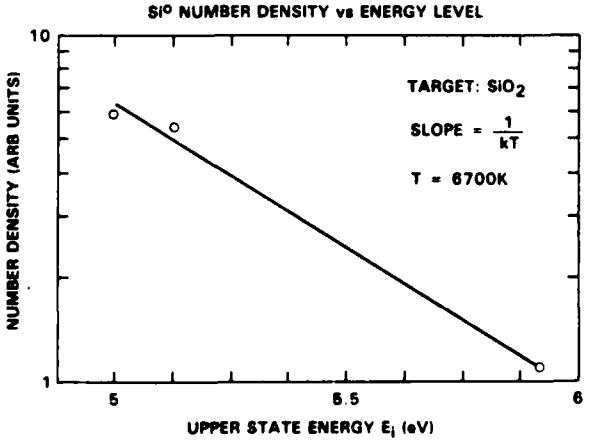

FIG. 5. Same as Fig. 4 for Si^0 in the evaporant plume of SiO.

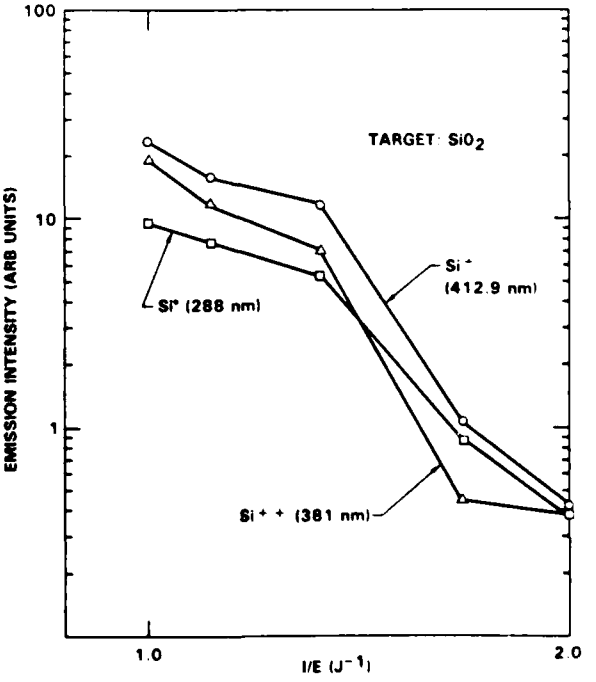

FIG. 7. Same as Fig. 6 for Si species in the evaporant plume of SiO.

the increase in excited Si species concentration with laser fluence.

To determine the effect of the laser pulse tail on the luminescence spectrum, the energy content of the tail was reduced to a negligible value by eliminating the N_2 from the laser gas mixture. Total energy of this pulse was made equal to that of a pulse with a tail by adjusting the laser discharge voltage. The luminescence spectrum of Al_2O_3 at 12.5 J/cm^2 fluence level was found to be essentially unaffected by the presence or absence of a tail in the laser pulse.

C. Molecular lines

Molecular emission bands were observed only for Al_2O_3 sources when radiated under high-vacuum conditions (10^{-7} Torr) (Fig. 8). These red degraded bands are attributed to the $\Delta v = 0$ progression of the $B\,^2\Sigma^+ - X\,^2\Sigma^+$ transition in AlO. Several very strong atomic lines were superimposed on the weak molecular bands, making vibration distribution measurements impossible.

The intensity of the molecular emission band increased with gas pressure as shown in Fig. 9, but the distribution of vibrational states did not change with gas pressure. Unexpectedly, the molecular emission band intensity was enhanced not only in the presence of O_2 but also in the presence of other gases, namely, He, N_2, and Ar at comparable pressures.

D. Effect of ambient gases

Experiments carried out in the presence of a gas showed that the evaporant plasma interacted with the gas in the chamber and produced discharge in the gas. Photographs of the plasma taken with various filters indicated a luminous core adjacent to the target surface surrounded by one or two pale envelopes for all materials tested. In general, the relative and absolute intensity of the lines of the target material did not change as much with gas pressure as the intensity of atomic lines of the ambient gas (e.g., Ar). The latter increased monotonically with pressure (Fig. 10).

The possibility that the plasma in the ambient gas may be due to the breakdown in the gas directly by the high electric field of the laser radiation was tested. No fluorescence associated with breakdown was observed in the gas in the absence of a solid target even under the highest pressures (0.2 Torr) and highest energy densities used in the experiments. The possibility of lower gas breakdown threshold in the vicinity of a solid surface was also investigated. To this end, nonabsorbing solid targets consisting of polished Al disks and Si wafers were used. In high vacuum and at 20 J/cm^2 incident energy, many of the neutral and some ionized species of the metal atoms were observed albeit at lower intensities than in the spectra of their respective oxides. When O_2 gas was introduced, excited O_2 species were observed only when metal (Al or Si) species were present in the plasma. Hence, we conclude that injection of excited or ionized solid target atoms are necessary for initiating the gas breakdown.

IV. DISCUSSION

In this work, optical techniques were used to analyze the plasma luminescence generated when an absorbing dielectric material is evaporated by a pulsed laser. Results indicate that optical breakdown in the evaporating target as well as absorption of radiation by the evaporating plume at high fluences produce numerous excited and ionized species. The resultant high temperatures cause dissociation so that only very weak molecular emission is observed in vacuum. Below, we discuss some aspects of the results as well as relevance of the present work to thin-film growth.

The dependence of the intensity of molecular band emission on the gas pressure and virtual independence on the gas species indicate that the collisions in the gas phase promote this emission in the vicinity of the surface. Pending further experiments, it is not known whether this enhancement is due to the collisional cooling of the plasma that would allow gas phase formation of the molecular species, or whether the slowing of the plasma expansion front in the presence of any gas allows emission of longer lived molecular species that would normally escape the detection area before relaxing to the lower energy state. Because AlO lifetimes (τ) are relatively long {e.g., τ[AlO($v' = 0$ to $v'' = 0$ transition)] = 236 ns}[13] and the velocities of many species are relatively large ($V_{ion} = 2 \times 10^5$ cm/s), the possibility that molecular species

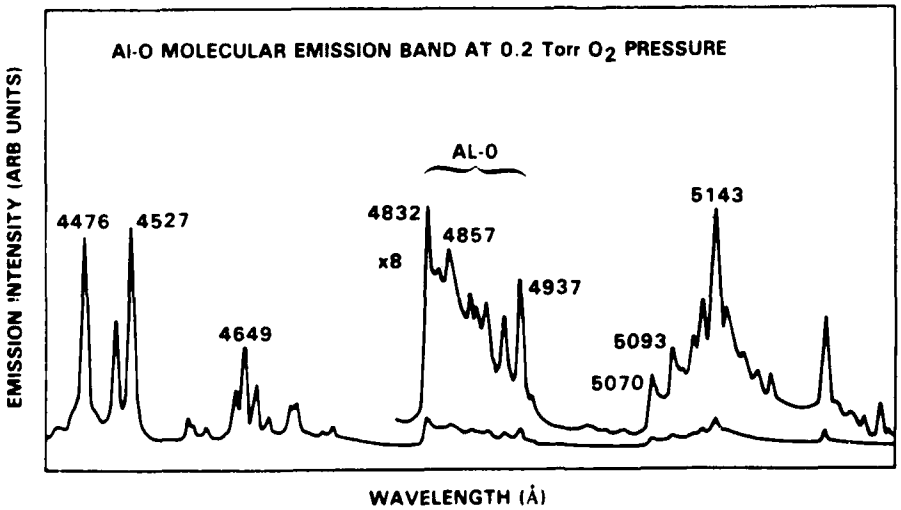

FIG. 8. Luminescence spectrum of the molecular emission band in the evaporant plume of Al_2O_3 in the presence of 0.2 Torr of O_2. Fluence is 20 J/cm^2.

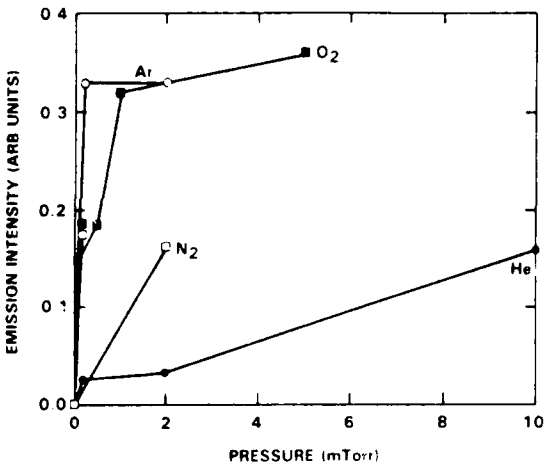

FIG. 9. Ambient gas pressure dependence of the molecular band emission intensity for Al-O ($B^1\Sigma \rightarrow X^1\Sigma$) in the evaporant plume of Al_2O_3. Fluence is 20 J/cm.

may escape the optically sampled volume (within 2 cm of the target surface) must be considered. To answer the above question the emission from a larger volume must be sampled.

The feasibility of reactive evaporation where the plume excites the ambient gas (see results above) is worth considering. The high pressures necessary to initiate a plasma in the host gas will cause excessive scattering of the evaporants, possibly rendering this method impractical. On the other hand, the above opens the possibility of depositing a thin film out of a plasma "collisional zone," as described in Ref. 14. In this case, the collision of two intersecting evaporant plumes produces a high-density region out of which material condenses on a surface placed across the bisector of the directions of the plumes. Solid particulates and molten droplets are not scattered by the high-density region and, therefore, avoid impinging on the substrate.

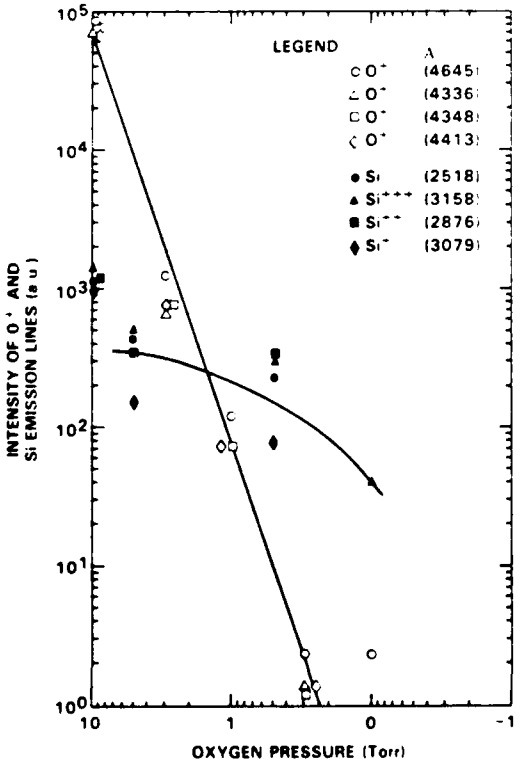

FIG. 10. O_2 pressure dependence of the O and Si emission line intensities. The target is SiO_2, ambient gas is O_2, and the laser fluence is 20 J/cm^2.

Preliminary experiments indicate that the emission spectrum of the plume does not depend on the absence or presence of the pulse tail, so long as the total energy of the pulse remains the same. Since the pulse tail may contain up to one-half of the total energy at less than 100th the power of the spike, we conclude that in the low fluence regime ($\lesssim$20 J/cm^2), the energy of the pulse determines the spectral characteristics of the plume.

The results indicate that the laser-vaporized material plume contains many species with energies well above that given by the equilibrium thermal evaporation. Furthermore, the laser fluence as well as the type of laser offer some degree of control on the type and energy distribution of the energetic species. The energetic component of the vapor plume is known to affect the properties of thin films deposited by various techniques.[15–17] This is due to the atomic reordering at the growth surface because of enhanced adatom mobility. The precise roles of the ions, energetic neutrals, excited species, UV and visible radiation, or the possibility of their synergistic effect are not yet fully known.

While the atomic species will not reach the thin-film substrate in their excited states due to their short lifetimes (order of nanoseconds) and due to large source–substrate distances (decimeters), many ions, metastable species, and excited molecular species will reach the substrate carrying electronic and kinetic energies. Experiments are underway to investigate the specific role of these species on the film properties of several dielectric materials.

Our sampling technique spatially averages a volume of about 2 cm^3. Calculations and experimental results of previous investigators indicated the spatially nonuniform nature in the laser-induced plasma of an evaporant plume. Experiments are underway to determine the extent of uniformity of the plume in our case. In the application of laser-induced evaporation to deposit thin films, the plume nonuniformity is likely to have little effect because of substrate rotation and variations in the orientation of the plume axis due to target surface irregularities.[18]

ACKNOWLEDGMENTS

This work was done under AFOSR Contract No. F49620-84-C-0091. The authors gratefully acknowledge D. Benard for the loan of OMA, M. Khoshnevisan for technical discussions, and D. Matthews for his technical assistance.

[1] R. Messier, A. P. Giri, and R. A. Roy, J. Vac. Sci. Technol. A 2, 500 (1984).
[2] P. S. Vincett, W. A. Barlow, and G. G. Roberts, J. Appl. Phys. 48, 3800 (1977).
[3] J. T. Cheung, G. Niizawa, P. J. Moyle, N. P. Ong, B. Paine, and T. Vreeland, Jr., J. Vac. Sci. Technol. (to be published).
[4] J. T. Cheung, Mater. Res. Symp. Proc. 29, 301 (1984).

[5]J. E. Rothenberg and G. Koren, Appl. Phys. Lett. **44**, 664 (1984).
[6]P. E. Dyer, S. A. Romsden, J. A. Sayers, and M. A. Skipper, J. Phys. D **9**, 373 (1976).
[7]V. P. Ageer, A. J. Borchukov, F. V. Bunkin, V. I. Konov, S. B. Puzhaev, A. S. Silenok, and N. I. Chaplier, Sov. J. Quantum Electron **9**, 43 (1979).
[8]Y. S. Touloukian and D. P. DeWitt, *Thermal Radiative Properties of Nonmetallic Solids* (1972).
[9]A. R. Streganov and N. S. Sventitski, *Tables of Spectral Lines of Neutral and Ionized Atoms* (1968).
[10]Reference in *Bibliography of Atomic Transition Probabilities*, Natl. Bur. Stand. Publ. No. 320 (U.S. GPO, Washington, DC).
[11]R. S. Adrain and J. Watsen, J. Phys. D **17**, 1915 (1984).
[12]Y. V. Afanasyev, O. N. Krokhin, and G. V. Sklizkov, IEEE J. Quantum Electron. **2**, 483 (1966).
[13]T. Wentink, N. Pedersen, and G. Diebold, ARPA Report No. DA-SA2704, 1971.
[14]S. V. Gaponov, A. A. Gudkov, and A. A. Fraerman, Sov. Phys. Tech. Phys. **27**, 1130 (1982).
[15]T. Ishida, S. Wabo, and S. Ushio, Thin Solid Films **39**, 227 (1976).
[16]D. Lubben, S. A. Barnett, K. Suzuki, S. Gorbatkin, and J. E. Greene, J. Vac. Sci. Techol. **63**, 968 (1985).
[17]H. Sankur, W. J. Gunning, and J. DeNatale, J. Vac. Sci. Technol. (to be published).
[18]H. Sankur and R. H. Hall, Appl. Opt. **24**, 3343 (1985).

6.3 Dense crystalline ZrO_2 thin films deposited by pulsed-laser evaporation

H. Sankur, J. DeNatale, W. Gunning, and J.G. Nelson

Dense crystalline ZrO_2 thin films deposited by pulsed-laser evaporation

H. Sankur, J. DeNatale, W. Gunning, and J. G. Nelson
Rockwell International Science Center, Thousand Oaks, California 91360

(Received 10 November 1986; accepted 10 May 1987)

A TEA-CO_2 laser was used to evaporate solid targets of ZrO_2 at power densities of 0.25 to 1.5×10^9 W/cm^2. The laser-generated plasma contained ions with velocities in the 2–6 $\times 10^6$ cm/s range. This ion flux normal to and 7.5 cm away from the solid source was in the range of 0.25 to 2.5×10^{14}/cm^2/laser pulse for the above power density range. ZrO_2 thin films deposited by this technique were characterized for their optical and structural properties. Under a broad range of laser power densities, these films had bulklike refractive index values, low absorption, and oriented polycrystalline microstructure.

I. INTRODUCTION

Many novel thin-film optical devices have stringent requirements on their optical performance and must survive in severe environments. This has driven the development of processes for depositing reproducible, stable, hard, stress-free films that are also invariant with environmental conditions. These desirable film properties are associated with bulklike properties of the material at hand. The films obtained by conventional physical vapor deposition methods contain voids, grain boundaries, and various other structural defects that are responsible for the less than ideal characteristics of the films.[1,2] High-temperature processes, such as chemical vapor deposition or postdeposition annealing and sintering, can produce dense films with large grains. However, high-temperature processes also promote undesirable chemical reactions, diffusion, or segregation; phenomena which may destroy the compositional profile of multicomponent films.

Recently, several low-temperature (< 300 °C) and high-vacuum techniques have produced dense, high-optical-quality films.[3–5] These techniques are based on bombardment of the growth surface with energetic particles during deposition. Pulsed-laser-assisted evaporation is one such technique that offers a unique combination of advantageous features.

The advantages of laser-assisted evaporation are (a) the production of ionized and excited species with high kinetic energies, (b) possibility of evaporating numerous compounds congruently with negligible heating of the target, (c) instantaneous control of the evaporation process, and (d) high-vacuum compatibility.

Laser-assisted evaporation for the deposition of optical and semiconductor films with properties comparable to those made by conventional techniques has been previously reported.[6–9] In these investigations cw (CO_2) or pulsed (ruby, Nd:YAG or excimer) lasers were used with energy densities in the 10^5–10^8 W/cm^2 range.

In this work, a TEA-CO_2 laser was used to evaporate ZrO_2 and other dielectric materials. The power densities were in the 0.25–1.5 $\times 10^9$ W/cm^2 range. The interaction of the laser beam with the evaporation target was found to generate a plasma in the evaporant stream containing high-kinetic-energy ions. ZrO_2 films grown from this plasma were found to have bulk index values and optical properties that were environmentally stable. The improved structural properties were attributed to the energetic ionized species found in the plasma.

II. EXPERIMENTAL

The deposition runs and plasma characterization experiments were performed in a vacuum chamber with a base pressure of 10^{-8} Torr. The chamber was fitted with mirrors and infrared transmissive windows and lenses to direct the laser beam onto the targets.

A Lumonics 820 TEA-CO_2 laser was used in multimode operation with ~3 J pulse energy. An antireflection coated ZnSe lens focused the beam to produce fluence levels of 15 to 200 J/cm^2. For comparison with films grown at low laser power, an 80-W cw CO_2 laser was also used to evaporate the ZrO_2 target. In some experiments, both lasers were used to evaporate the same area of the source or each laser was used concurrently on different sources.

The temporal behavior of the laser output was characterized using a Molectron pyroelectric detector. Laser power was monitored using a Gentech energy meter.

ZrO_2 evaporation grade sintered pellets were used for plasma and thin-film deposition studies. Several other materials listed in Sec. III were also used during some phases of plasma studies.

The laser-induced plasma was characterized by means of a Faraday cup. Temporal behavior of the ion current was observed on a fast oscilloscope. The spatial distribution of the ionized species was measured by rotating and translating the Faraday cup with respect to the source. Current was monitored using a probe biased at -100 V. Measurements taken at lower bias voltages indicated that the time of arrival of the peak ion flux did not vary with voltage and that the ion current saturated at about 70–80 V. Data on the temporal behavior of the ion current were used to calculate the total charge impinging on the surface area of the probe.

Films were deposited on room-temperature substrates of glass, silicon, GaAs, and NaCl. A thermocouple on the substrate holder monitored any temperature rise due to radiation from the source or the plasma. Chamber pressure was maintained at 10^{-4} Torr of O_2 in some deposition experiments. The typical film thickness was 2000 Å.

Thin ZrO_2 films were deposited at a source-to-substrate

 0734-2101/87/052869-06$01.00

separation of 7.5 cm. At this distance the deposition rate is ~0.15 Å/(laser pulse) resulting in ~100 Å/min rate for a laser pulse rate of 10 Hz.

Thermal radiation from the source material was very small, resulting in a 10–15 °C rise of substrate temperature. This was due to low average laser power (20 W) and small area of the evaporation zone. For smaller source-to-substrate distances, there can be some heat transfer directly from the plasma. Experiments where the temperature rise of a small Cu block suspended in the vicinity of a laser-generated plasma was measured indicated that such heat transfer can be important for distances of less than ~3–4 cm from the source.

Optical properties were determined by spectrophotometric analysis and ellipsometry. Structural properties were studied using x-ray diffraction and transmission electron microscopy (TEM). Film morphology was analyzed using optical and scanning electron microscopy. Some films deposited on metallized substrates were tested in chemical etches to observe integrity and density of the pulsed-laser-evaporated films.

III. RESULTS

A. Plasma properties

Interaction of the pulsed CO_2 laser radiation with the source material induced a plasma in the evaporant plume near the surface of the evaporation target and produced copious amounts (20 A/cm^2 at 7.5 cm from the source) of energetic ions. This plasma was observed qualitatively to have high emission luminosity. Spectroscopic analysis of laser induced plasmas in other absorbing dielectrics had indicated the presence of highly excited neutral, singly, and doubly ionized species.[10] Such analysis was not done in the present study. Below we present the results of the electrical analysis of such plasmas.

B. Ion velocities

A translatable Faraday cup was used to measure the density and velocity of the ions in the evaporant plume. Typical temporal behavior of the ion current for ZrO_2 is shown in Fig. 1 for a laser fluence of 63 J/cm^2 with laser pulse shapes consisting of a 100-ns pulse followed by ~1-μs tail. One high-velocity and two lower-velocity species (labeled as A, B, and C) are observed for ZrO_2 and most other oxides that were analyzed by this technique.

The velocities are derived from the slopes of the curves representing time of arrival of peak ion current versus probe-to-source distance. This approach eliminates the ambiguity in the determination of the origin of time. Figure 2 shows such a plot for the species indicated in Fig. 1.

The velocities derived from the slopes in Fig. 2 are 5.77, 2.76, and 2.35×10^6 cm/s for peaks labeled A, B, and C, respectively. The velocity of the peak labeled as A is about 25 to 50 times larger than the calculated thermal velocity of atomic species (Zr or O) emanating from an evaporating ZrO_2 source at ~5000 °C.

In some experiments the laser pulse tail was considerably reduced by eliminating N_2 gas in the laser gas mixture. When the integrated laser energy output was adjusted to be the same as for pulses with tails, the ion spectrum consisted only of the high-velocity species. Apparently, the two low-velocity species are generated due to the interaction of the pulse tail with the solid or the plasma in the evaporant plume generated by the spike part of the pulse.

To investigate the origin and nature of the laser-generated plasma, other materials, including several oxides, were used

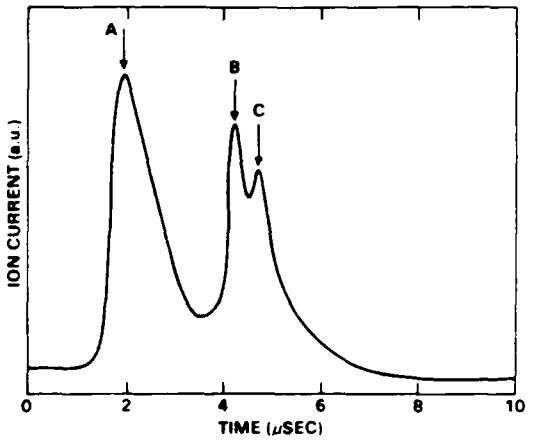

FIG. 1. Ion current vs time in the plasma generated by a TEA-CO_2 laser incident on a ZrO_2 evaporation target. Fluence is 63 J/cm^2 and the current probe is 7.5 cm away from the target.

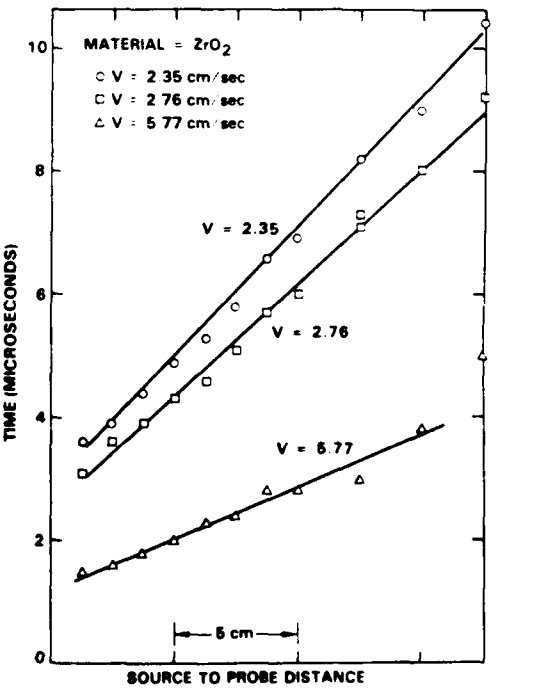

FIG. 2. Time of arrival of peak ion flux vs source-to-probe distance. Conditions are the same as in Fig. 1. The velocities are calculated from the inverse of the slopes. The curves do not intersect the time axis at $t = 0$ because the time of arrival data have an arbitrary time delay.

as evaporation targets. These materials were Al_2O_3, TiO_2, MgO, ZnO, Ta_2O_5, Si, C, ZnS, ZnSe, and CaF_2. Ion velocities from these materials were also in the $2-10 \times 10^6$ cm/s range. The measured velocities exhibited a very weak dependence on atomic mass with a general trend toward lower velocities for higher masses. The ratio of velocities between the lightest and heaviest cation compound was 1.35, whereas the ratio of the masses was 7.65.

The dependence of ion velocities on fluence for a ZrO_2 target is shown in Fig. 3. This dependence can be expressed as $v = F^{1.5}$ where F represents the laser fluence for all velocity species.

C. Ion flux

Ion flux was measured as a function of fluence, probe-to-source distance, and cw laser heating of the evaporation target.

The dependence of integrated ion current on fluence (in essence total charge per laser pulse normal to the source) is shown in Fig. 4 for ZrO_2. As expected, the total charge increases with laser energy per unit area. The peak ion currents, when measured 7.5 cm away from the source, were in the 0.18–15 A/cm^2 range for laser fluences between 25 and 160 J/cm^2.

The ionized particle flux for maximum laser energy fluence at a 10-Hz pulse rate is calculated to be 2×10^{15}/cm^2/s. In converting measured current to ion flux, only singly charged ions are assumed to exist. Since singly, doubly, and even triply ionized particles are known to be present in the evaporant plume of many absorbing dielectric materials,[8] the above ion flux is certainly overestimated, perhaps by as much as a factor of 2. On the other hand, the particle flux calculated from the deposition rate is only 4.5×10^{14} cm^2. Since even the ionized portion of the evaporant flux is larger than the deposition rate, reduced sticking coefficients and self-sputtering must play roles in the deposition process.

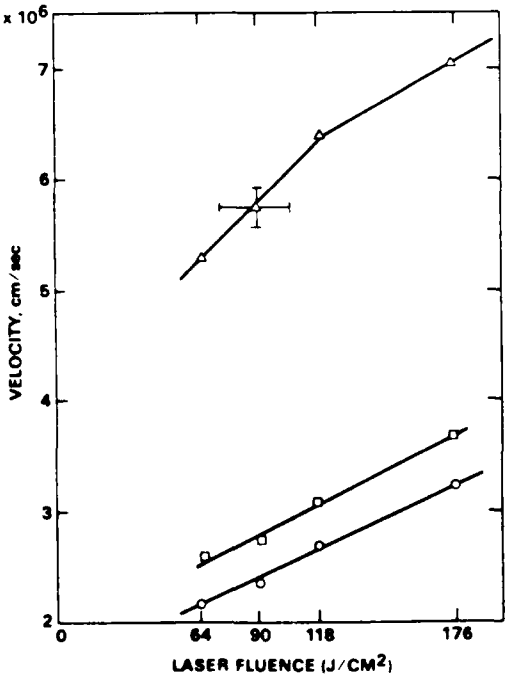

FIG. 3. Velocity of the species labeled as A, B, and C in Fig. 1 vs laser fluence.

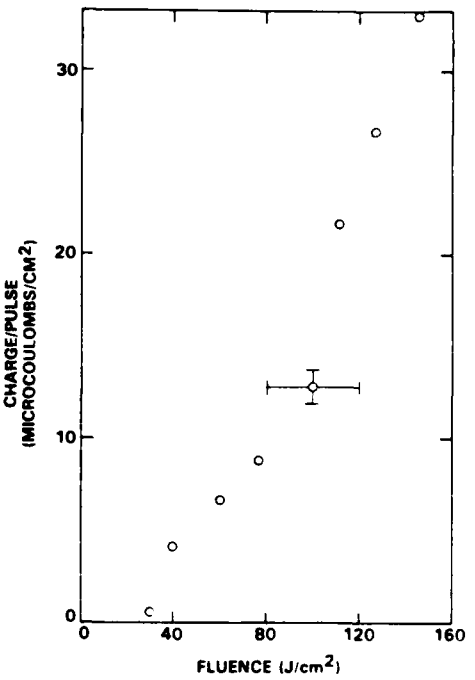

FIG. 4. Integrated total ion charge vs laser fluence.

Both the total charge flux (q) and deposition rate (r) vary inversely with distance (d). This dependence can be expressed as q (or r) $= d^{-2.5}$ when measured normal to the source surface. The fact that the charge flux and the evaporant density vary with the same dependence on distance indicates that the plasma is in a state of noncollisional expansion with no detectable charge neutralization for distances greater than 7.5 cm from the source.

In some experiments, an 80-W cw laser was used to simultaneously heat the evaporation zone. The effect of this on the ion current spectrum was small even at the highest cw power levels, where some evaporation of ZrO_2 due to cw laser heating took place. The high-velocity ion component decreased and the low-velocity ion components increased by a factor of 2.

IV. THIN-FILM PROPERTIES

A. Optical properties

The optical properties of the thin ZrO_2 films grown by pulsed-laser evaporation under 1×10^{-4} Torr of O_2 pressure were found to be comparable to bulk values. Film refractive indices were in the 2.13–2.17 range at 632.8 nm and typical extinction coefficient was $k = 0.001$. These values were obtained for all laser fluences between 0.25 and 1.5×10^{7} W/cm^2. By way of comparison, cw laser-evaporated films had index values of 1.85 to 1.93.

The extinction coefficient of the films grown in 10^{-7} Torr of pressure was found to depend on the fluence. High-fluence (F) laser radiation ($F > 1 \times 10^9$ W/cm^2) produced films that had higher extinction coefficients. These films were light brown in color suggesting O_2 deficiency. Backfilling the vacuum chamber with 1×10^{-4} Torr of O_2 resulted in clear films with very low absorption.

In order to clarify the role of the ions, depositions with concurrent cw and pulsed laser evaporation of ZrO_2 targets were carried out. A focused cw laser beam at 6000 W/cm^2 and a pulsed laser beam at 3×10^9 W/cm^2 were incident on separate parts of the source material. The deposition rate due to cw laser heating [r(cw)] was maintained at 1.5 Å/s while that due to pulsed-laser heating [$r(p)$] was varied from 0.015 to 1.5 Å/s. Figure 5 shows the variation of index with relative pulsed-laser evaporation rate

$$r = \{r(p)/[r(p) + r(\text{cw})]\}.$$

For relative rates of 0.13 and above, corresponding to 1.5-Hz pulse frequency, essentially bulk index values are obtained. These results indicate that the deposition of high-density films can be carried out by cw laser, or even electron beam assisted evaporation, with periodic pulses of high-kinetic-energy ions. The minimum pulsed evaporation rate which resulted in a refractive index of 2.15 corresponded to a charge flux of 42.5 μC/cm^2/s or 2.65×10^{14} ions/cm^2/s.

B. Structural properties

Selected area diffraction and convergent beam microdiffraction established the crystalline phase as the monoclinic ZrO_2 structure for all pulsed-laser evaporated films. These crystals exhibited a high degree of preferential orientation about the (100) zone axis. This orientation relation is not simply due to interactions with the sodium chloride substrate but has been observed, by x-ray diffraction, to occur on amorphous glass substrates as well. Electron diffraction patterns from the regions between the crystallites exhibited distinct broad maxima rather than the diffuse halo typical to truly amorphous structures. This indicates that even in the noncrystalline regions of the film, some degree of short-range ordering is present.

While the microstructures of the room-temperature films were qualitatively similar, there was a distinct dependence of crystallite size on the laser fluence. Very fine crystals (~20 nm) were formed at the low fluence values of 28 J/cm^2. At a fluence of 50 J/cm^2 the crystalline regions had increased to an average size of 110 nm. Increased fluence levels of 123 J/cm^2 produce still larger crystallite sizes (average size of ~220 nm). Representative microstructures for these laser fluences are compared in Figs. 6(a)–6(c).

The temperature of the substrate also had a dramatic influence on the microstructural development of these films. Comparative films were deposited on room-temperature and 300 °C substrates, respectively, using a constant laser fluence of 28 J/cm^2. The higher substrate temperature induced a substantially higher nucleation rate and caused complete conversion of the film to the crystalline structure [Fig. 6(d)]. This increased temperature did not, however, enhance growth of the crystallites, but rather led to a significantly lower average grain size of ~10 nm.

The dense nature of ZrO_2 films grown by pulsed-laser evaporation was also ascertained qualitatively when these were tested as a protective capping layer for metallic films. 800-Å-thick ZrO_2 films were deposited on Au and Al films and immersed in concentrated aqua regia and hydrochloric acid, respectively. The metallic films capped by cw laser-evaporated ZrO_2 dissolved in minutes, whereas those capped by pulsed-laser-evaporated ZrO_2 did not show signs of degradation even after 24 h.

C. Particulates

Pulsed-laser evaporation produces particulates, some of which become embedded in the film. In our studies of ZrO_2 thin-film deposition, the size and density of such particulates

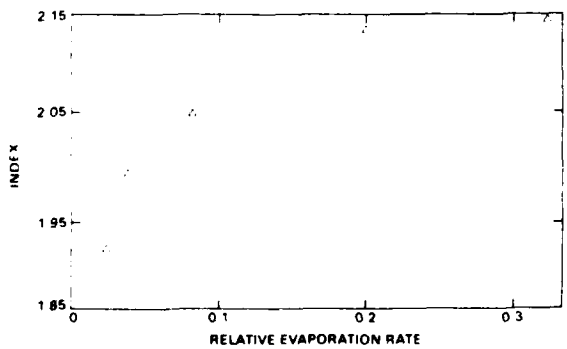

FIG. 5. Refractive index of ZrO_2 thin films deposited by concurrent cw and pulsed-laser evaporation vs the relative evaporation rate $r = (r_p/r_{cw} + r_p)$. r_p and r_{cw} are the pulsed and cw laser evaporation rates, respectively.

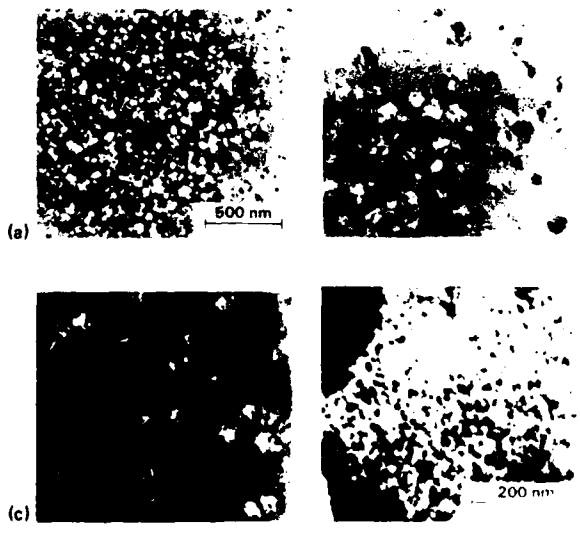

FIG. 6. (a), (b), (c) TEM micrographs of ZrO_2 thin films deposited by pulsed-laser evaporation. (a), (b), (c) refer to films deposited at 28, 50, and 128 J/cm^2 fluence respectively. Note the increase in crystallite size. (d) TEM micrographs of ZrO_2 thin films deposited on 300 °C substrates by pulsed-laser evaporation at 28 J/cm^2 fluence.

were observed to depend on laser fluence.

At the highest fluences ($> 100\ J/cm^2$), 3–5 μ size spherical or disk-shaped particulates, indicative of molten droplets, were observed on the film surface. The density of these was $3–10/mm^2$.

At the lowest fluences ($< 40–50\ J/cm^2$) large numbers of irregularly shaped submicron-size solid particulates ($\sim 100–1000/mm^2$) covered the surface. However, in films grown at intermediate laser fluences (50–100 J/cm^2) no molten droplets and a lower density ($10–100/mm^2$) of solid particulates, 0.1–0.3 μm in size, were observed. The origin of particulates is probably fracturing of the solid via a thermal pulse induced by the laser. Particle ejection is caused by partial vaporization of the particulates or by rapid evolution of gas at the surface. At intermediate fluences where low particulate density is observed it is conjectured that small particulates that are produced at the surface of the source material are completely vaporized and that laser heating does not cause a large melt pool to form from which droplets can be ejected.

When the evaporation zone was also irradiated with a cw laser beam ($6000\ W/cm^2$), the number of solid particulates did not change but spherical droplets appeared, indicating formation of a larger melt pool.

The effect of the particulates on the optical properties of the film was not detectable to within the accuracy of the data. Scattering was not measured in these studies. In future studies, mechanical particle deflectors will be used to further reduce the particulate density.

V. DISCUSSION

A. Electrical properties of the plasma

Interaction of the high fluence, pulsed-laser radiation with a solid target and with the ensuing vapor plume produces ionized, energetic, and highly excited species.

Ionic species have been reported by other investigators during laser-induced evaporation of solids at much lower fluences.[11,12] However, the measured velocities of the species were given by the Maxwell–Boltzmann distribution corresponding to the evaporation or sublimation temperature of the solid. In other reports[13] of experiments done at higher fluences, a "thermal" neutral atom pulse followed the initial "nonthermal" ion pulse when easily vaporizable materials were used. In the case of refractory ZrO_2, such is not expected to be the case owing to the high energy of sublimation of the compound. In fact, when an ionizer placed in front of the Faraday cup was turned on, no detectable ion pulse, other than that due to the plasma ion current, discussed earlier, was observed.

Free expansion of the dense plasma formed at or near the solid surface, and absorption of part of the laser pulse by this plasma via inverse bremsstrahlung, have been proposed as the likely mechanisms of imparting high kinetic energies to the species.[14–16] In our experiments, ions in the same velocity range ($1–10 \times 10^6$ cm/s), and with roughly comparable fluxes, were produced from all the materials tested. Some of these materials (ZrO_2, Ta_2O_5, C, TiO_2, Al_2O_3, MgO, ZnO) were absorbing for 10.6-μ radiation and others (Si, ZnS, ZnSe, CaF_2) were not. These results suggest dielectric breakdown at the solid surface as the mechanism for plasma generation for which the optical and thermal properties of the materials would not be as important.

Our experiments also indicated that the low-velocity species, labeled as B and C, are due to the presence of the tail in the pulse. The power density of the tail is roughly a factor of 100 smaller than that of the peak. If the high-velocity curve (A) is extrapolated to lower fluences, the resulting velocities are found to be in the $1–2 \times 10^6$ cm/s range suggesting that the tail may be creating its own plasma at the solid surface (preheated by the spike part of the pulse).

The velocity spread (Δv) was found to be smaller than the absolute value of the velocity (v) with typical values of their ratio ranging from 0.5 to 0.7. This indicates low translational gas temperature is obtained in a freely and adiabatically expanding plasma. Here, the expansion removes the energy of the relative translations of the atoms, in effect "cooling" the plasma.

The kinetic energies of the particles cannot be estimated accurately without determining the masses of the species. Pending mass spectroscopic analysis, an upper limit of 1560 and 275 eV is obtained for Zr and O atoms for high-velocity species. These energies are in reasonable agreement with data reported by other investigators for the same fluence range.[17] The corresponding energies for the lower-velocity species are 265 and 45 eV, respectively.

B. Thin-film properties

ZrO_2 films grown by pulsed-laser evaporation were found to be dense and to have bulklike optical properties. Many of the results of pulsed-laser evaporation are similar in nature to the recently published results of ion assisted deposition (IAD) of optical coatings.[3] The IAD films are typically bombarded by a 600-eV ion current of 40 to 100 $\mu A/cm^2$. In our case the average ion current was in the range of 43 to 290 $\mu A/cm^2$. The effect of bombarding of the film growth surface by energetic ions is to densify and promote crystallinity of the films by enhancing adatom mobility and by other mechanisms.[18]

The dramatic microstructural difference between high-fluence low-temperature deposition and low-fluence high-temperature deposition underscores the conclusion that substrate heating is negligible, even at the highest laser fluences. The nucleation-dominated microstructure characteristic of high thermal mobility is absent in all of the room-temperature films. The increased ion energies at the higher laser fluences do, however, enhance atomic transport to the extent of increasing crystallite growth in the films.

VI. CONCLUSION

Pulsed laser-assisted deposition is different from conventional and even cw laser-assisted evaporation. Pulsed-laser evaporation produces controllable amounts of high-kinetic-energy ions as well as excited states in the evaporant particles. This is one of the important advantages of the laser-assisted deposition technique.

It has been shown that the ions in the laser-induced plas-

ma promote crystallinity as well as good optical properties representative of dense bulklike material in thin films of ZrO_2 deposited by this technique.

In pulsed-laser evaporation, the rate of evaporation, ion energy and ion flux for a given material are not completely decoupled as in the case of IAD. However, varying the pulsed-energy density while maintaining constant pulse energy has been proven to provide independent control of the rates of ion and evaporant production.

Judicious use of laser fluence was shown to produce films with few particulates. We are currently investigating several alternative methods to further reduce or eliminate particulates.

Pulsed-laser evaporation is likely to be a practical technique of thin-film deposition with advantageous features for some materials.

ACKNOWLEDGMENTS

The authors gratefully acknowledge Dr. K. Malloy for his fruitful comments and his support through AFOSR Contract No. F49620-84-C-0091.

[1]K. H. Guenther, SPIE Proc. **401**, 31 (1983).
[2]H. A. Macleod, SPIE Proc. **325**, 21 (1982).
[3]P. J. Martin, J. Mater. Sci. **21**, 1 (1983).
[4]J. R. Sites, P. Gilstrap, and R. Rujkorakarn, Opt. Eng. **22**, 447 (1983).
[5]T. Takagi, I. Yamada, K. Matsubara, and H. Takaska, J. Cryst. Growth **45**, 318 (1978).
[6]J. T. Cheung, G. Niizawa, J. Moyle, N. P. Ong, B. M. Paine, and T. Vreeland, Jr., J. Vac. Sci. Technol. A **4**, 2086 (1986).
[7]H. Sankur and E. Motamedi, IEEE Ultrasonics Symposium Proceedings, Atlanta, 1983, p. 316.
[8]S. V. Gaponov, B. M. Luskin, B. A. Nesterov, and N. N. Salaschenko, Sov. Phys. Solid State **19**, 1736 (1977).
[9]D. Lubben, S. A. Barnett, K. Suzuki, S. Gorbatkin, and J. E. Greene, J. Vac. Sci. Technol. B **3**, 968 (1985).
[10]H. Sankur, J. G. Nelson, A. T. Pritt, Jr., and W. J. Gunning, J. Vac. Sci. Technol. A **5**, 15 (1987).
[11]G. P. Schwartz, V. E. Bondybey, J. M. English, and G. J. Guoltieri, Appl. Phys. Lett. **42**, 952 (1983).
[12]P. S. P. Wei, D. J. Nelson, and R. B. Hall, J. Chem. Phys. **62**, 3050 (1975).
[13]A. T. Prengel, J. Dehaven, E. J. Johnson, and P. Davidovits, J. Appl. Phys. **48**, 3551 (1977).
[14]H. Weichel and P. V. Avizonis, Appl. Phys. Lett. **9**, 3334 (1966).
[15]K. Dick, H. Pepin, J. Martineau, K. Parbhoker, and A. Thibandeau, J. Appl. Phys. **44**, 3284 (1973).
[16]O. Krokhin, in *Laser Handbook*, edited by F. T. Arecchi and E. O. Schulz Dubois (North-Holland, Amsterdam, 1972), p. 1371-1407.
[17]S. V. Gaponov and M. D. Strikorskii, Sov. Phys. Tech. Phys. **27**, 1127 (1982).
[18]T. Takagi, Thin Solid Films **92**, 1 (1982).

END
DATE
FILM
4-88
DTIC